Physics – Uspekhi **46** (12) 1231 – 1252 (2003)

REVIEWS OF TOPICAL PROBLEMS PACS numbers: 34.50.Dy, **41.20.–q**, **41.60.–m**

High energy electromagnetic processes in amorphous and inhomogeneous media

M L Ter-Mikhaelyan

DOI: 10.1070/PU2003v046n12ABEH001368

Contents

Abstract. This review covers the results of experimental and theoretical investigations of radiative electromagnetic processes in amorphous and inhomogeneous media obtained after the monograph [1] came out. Bremsstrahlung with the inclusion of the Landau – Pomeranchuk effect, the longitudinal density effect, Ginzburg – Frank transition radiation, and other underlying effects are discussed. Also considered are radiative processes involving optical and γ-ray radiation occurring because of fluctuations of the medium parameters or other types of inhomogeneities in the passage of a uniformly moving charged particle through a medium. The review is intended for a wide circle of readers: experimenters, theorists, and senior students.

1. Introduction

The proposed review considers the problems of radiation by high-energy charged particles in Coulomb scattering in amorphous media. Apart from the well-known theoretical investigations and first experiments performed in the 1950s – 70s (see Ref. [1]), this direction has recently given rise to a flood of new theoretical and experimental investigations, which are of considerable interest for the physics of an energy range of tens and hundreds of gigaelectronvolts. Experimental research is underway in the world's largest accelerators at Stanford, CERN, etc., and the results obtained are discussed at numerous international conferences. The mathematical apparatus of theoretical works has been considerably augmented in recent years, which is helpful in studying more subtle effects (a more rigorous inclusion of screening and transition radiation, absorption, etc.).

In addition, the review places emphasis on the investigation of radiative processes arising from particles uniformly moving through inhomogeneous amorphous media that have been carried out in recent decades. These investigations underline the deep relationship between the radiative processes initiated by electromagnetic radiation, on the one hand, and charged particles on the other. They have a direct bearing on the investigation of substance properties and have attracted considerable recent attention. We also mention investigations of charged-particle beam structure with the use of transition and diffraction radiation in the optical range. Also discussed is the emission of hard X-ray photons by particles uniformly moving through inhomogeneous amorphous media and a comparison is made with similar effects in periodic structures, which were considered at length in the previous review [2].

2. Coherence length

The effect of the medium on electromagnetic processes was expounded in a monograph [1], which summarized the theoretical and experimental accomplishments in this field made during the period 1953 – 1972. Naturally, we do not reproduce the material of monograph [1] in subsequent sections, in particular because it is still widely used by experts in high-energy physics. It might be well to point out that its publication has been followed by the appearance of many

M L Ter-Mikhaelyan Institute for Physical Research, Armenian Academy of Sciences, 378410 Ashtarak-2, Armenia
Tel. (7-374) 28 81 50. Fax (7-374) 323 11 72
E-mail: mikhael@ipr.sci.am

Received 19 November 2002, revised 11 June 2003
Uspekhi Fizicheskikh Nauk **173** (12) 1265 – 1286 (2003)
Translated by E N Ragozin; edited by A M Semikhatov

reviews, monographs, and textbooks that discussed the effect of the medium on high-energy processes. A list of them appears in the foreword to review [2], concerned with similar phenomena in crystalline media, and is not reproduced here.

Among the experimental works performed (after the publication of Ref. [1]) on the accelerators in Dubna and Serpukhov, which confirmed the influence of multiple scattering and the longitudinal density effect on the bremsstrahlung of relativistic particles in amorphous media, I would like to highlight only two papers: [3, 4]. The former ascertained the existence of the longitudinal density effect and the latter the existence of the Landau – Pomeranchuk effect.

Important experimental inquiries into these topics were made in the realm of cosmic rays. However, they are not discussed in my review because an adequate cascade theory of electron – photon showers (with the inclusion of suppression effects) has not been constructed to date. Nevertheless, experimental data obtained in the range of energies above the limit attainable with accelerators are undoubtedly of interest. The research in the realm of cosmic rays carried out prior to 1969 – 1970 is well represented in monograph [1]. In recent works related to the neutrino detection problem, advantage is taken of extended electron – photon showers caused by μ-mesons whose energy may be as high as 10^{24} eV. The results thus obtained are outlined in Refs [5a, b], which contain references to the preceding papers.

The year 1994 saw the implementation of experimental investigations of radiative processes in an amorphous medium performed by the SLAC E-146 collaboration of scientists from the Stanford Acceleration Center, the American University in Washington, D.C., the Institute for Particle Physics of California State University, and Lawrence Berkeley Laboratory. The results were reported by M L Pearl at a Conference in France [6] to immediately come to the attention of physicists engaged in high-energy physics. Experiments to measure the bremsstrahlung spectrum (in the 0.2 – 500 MeV range) were performed with a high precision at the Stanford Linear Accelerator with the electron energies 8 and 25 GeV. They confirmed the author's theoretical statement[1] that the high-directivity radiation of relativistic particles is formed throughout a coherence length, which can, for a high energy of the radiating particle or in the emission of soft photons, attain macroscopic dimensions

$$L_{\text{coh}} = \frac{2E_1E_2}{\omega m^2 c^3}\,, \tag{1}$$

where $E_{1,2}$ are the electron energies before and after the emission of a photon with a frequency ω, m is the electron mass, and c is the speed of light. Naturally, the specific form of formula (1) can be refined depending on the angle of photon emission, multiple scattering angles, the kind of particle, and other factors in the processes discussed below. In what follows, we frequently use the effective momentum corresponding to L_{coh}, which is transferred to the medium along the trajectory of the radiating particle and is commonly denoted as

$$\hbar\delta_{\text{coh}} \cong \frac{\hbar}{L_{\text{coh}}}\,. \tag{2}$$

This statement immediately leads to a fundamental conclusion: for very high energies (or very soft photons), when the coherence length exceeds the interatomic distance, considering the particle – substance interaction as the sum of independent interactions with individual atoms is illegitimate[2]. Roughly speaking, the atoms located within the coherence length along the particle trajectory act coherently, and therefore the probability of the corresponding physical process is proportional to the squared number of atoms within the coherence length. This statement was first made in 1953 (for more details, see the references given in footnotes 1 and 2). It implies that for certain processes, microscopic quantum electrodynamics should be replaced with (presently non-existent) macroscopic quantum electrodynamics. Several attempts to construct macroscopic quantum electrodynamics have already been made. In [7a], the example of the electron mass renormalization is considered with medium polarization effect taken into account (see Section 3 for more details), and the relevant publications existing at the time are listed. In the recently published Ref. [7b], the mass and anomalous magnetic moment of the electron were calculated with the inclusion of multiple scattering in the substance. According to the authors' estimates, the effect will be possible to observe at electron energies above 10^{12} eV in thin layers of substance made up of heavy elements.

Anthony et al. discuss the experimental results confirming the effect predicted by Landau and Pomeranchuk (the LP effect in the subsequent discussion) [10] and the effect predicted by the author of the present review [11], which is sometimes referred to as the longitudinal density effect, to distinguish it from the well-known Fermi density effect in the theory of ionization losses. Other terms are also frequently used: the medium polarization effect, the density effect, the dielectric suppression effect, or simply the TM effect.

The theoretical works of past years were based on Migdal's investigations [12a], who took both effects into consideration (see reviews [12b, c]). Migdal's expressions are commonly employed in the comparison with experimental data (the name LPM theory has survived in the literature). But even at that time, new theoretical papers appeared that were concerned with the investigation of other examples of how the medium affected radiative processes. These works extended the range of applicability of the Migdal theory by extending the consideration to the photon absorption, the transition radiation of a particle in a plate, the angular distribution and polarization of photons, the interference of different kinds of radiation in the medium, etc. (see Ref. [1] and references therein).

The level of experimental resources at that time was quite insufficient to obtain the required quantitative data and verify the theoretical calculations. A wealth of experimental investigations was performed in the study of extended air showers with subsequent comparison of experimental results with cascade curves calculated with the inclusion of the theoretical results given in Ref. [1] (references to the papers of the past years can be found in Refs [5, 6]).

After the publication of the first results [6, 8, 9], new research was undertaken and experimental data were compared with improved theories (see Ref. [13] and review [14]).

[1] Ter-Mikaelyan M L *Zh. Eksp. Teor. Fiz.* **25** 289, 296 (1953); see also Ref. [24, Sect. 93, p. 461].

[2] Feĭnberg E L "Effekt, podtverzhdennyĭ cherez sorok let" ("Effect borne out forty years later") *Priroda* (1) 30 (1994) [Translated into English: http://www.phys.au.dk/~ulrik/lpm/Nature.doc]; see also Akhiezer A I, Shul'ga N F *Usp. Fiz. Nauk* **151** 385 (1987) [*Sov. Phys. Usp.* **30** 129 (1987)].

We discuss theoretical works and compare them with experimental data in the ultra-high energy range in Section 4.

Recently (March, 2002), there appeared first reports about the experiments carried out by Uggerhøj's group at CERN [15] (private communication). The bremsstrahlung cross section was measured for the electron energies 149, 207, and 287 GeV. Unlike in the experiments performed in Stanford, in this case the spectrum was measured everywhere over the photon emission energy range. This enabled the authors of Ref. [15] to determine the energy losses in thin targets of iridium, tantalum, copper, and carbon and to show that the effective radiation length increases steeply at these energies (see below).

3. Graphic picture of suppression of radiative processes

The above examples point to the significant role played by the coherence length in electromagnetic radiation at ultrarelativistic energies [16–19]. Furthermore, it turned out that similar effects also occur in hadronic processes, i.e., in quantum chromodynamics (see, for instance, Refs [16–18, 20, 21] and references therein), which are now actively investigated. We can therefore say that some processes described by quantum electrodynamics or quantum chromodynamics involve a nonlocal interaction, because there is no way of specifying at what point within the coherence length the interaction occurred. This statement is fundamental in character, and we therefore enlarge on it, following the well-known review by E L Feĭnberg [18], who is the founder of this movement in high-energy nuclear physics and in quantum electrodynamics (see Ref. [16]).

According to modern quantum electrodynamics, the electron should be treated as a point particle. This leads to several difficulties, which may be overcome using special recipes (the renormalization theory). We try to explain them following the review [18], in which present-day problems of high-energy physics are outlined in a manner comprehensible to a broad circle of readers.

A nonrelativistic charged particle in the form of a ball of radius r_0 moving with an acceleration $\mathbf{r}''$ radiates energy and experiences the radiative friction force $(4/3)(e^2/\pi r_0)\mathbf{r}''$ directed oppositely to the radiation. It becomes infinite as the electron radius tends to zero. However, even in the 19th century, Lorenz noted that because the inertial force $m\mathbf{r}''$ is also proportional to the acceleration, it can be combined with the radiative friction force to introduce a new (renormalized) mass m, taking it to be equal to the mass of a real electron. In this case, the electron radius may subsequently tend to zero to obviate the emergence of infinities in the equations of motion.

A similar procedure should also be carried out to eliminate other infinities emerging in the quantum theory of electromagnetic fields. For instance, it is necessary to introduce a renormalized electron charge, because the Dirac theory implies an infinite background of negative-energy states that should be filled with electrons to eliminate the electron transition to unoccupied negative-energy levels with the emission of photons. The outer electron polarizes the background with the consequential screening of its charge, and hence the charge (which is the constant for coupling to the electromagnetic field) must also be renormalized. Lastly, the third infinite quantity emerging in the theory (the so-called vertex part) must also be renormalized to enable finite results to be obtained in quantum electrodynamics in the calculation of specific processes involving a point electron.

As a result of the renormalizations conducted, notwithstanding all the artificiality of this procedure, quantum electrodynamics describes all experimental data known to date with high precision, although it remains inconsistent from the logical standpoint.

However, assuming that the renormalization due to the interaction of a (nonrenormalized, i.e., bare) electron with other fields not included in quantum electrodynamics does not occur instantly (the relativity theory supposes that any velocity of signal transfer is limited by the speed of light) but takes a certain period of time, which is termed the proper field regeneration time, or simply the dressing time, we conclude that the bare (i.e., nonrenormalized) moving electron manages to travel some distance during the dressing time. The higher its velocity, the longer this distance.

We can attempt to estimate the regeneration time, remaining in the framework of the quantum theory [18]. By way of example, we consider an atom with only two levels (a two-level system) experiencing a periodic perturbation of the form $\mathbf{E}\exp(-\mathrm{i}\omega t) + \text{c.c.}$ We use the perturbation theory to derive the probability that the atom resides in the upper state at a time instant $t > 0$ assuming that it was in the lower level at $t = 0$. The answer is well known (see, for instance, Ref. [22]),

$$W_{21} = \left(\frac{2\mathbf{d}\mathbf{E}}{\hbar\Delta}\right)^2 \sin^2\frac{t\Delta}{2}\,, \tag{3}$$

where

$$\hbar\Delta = E_2 - E_1 - \hbar\omega = \hbar(\omega_{21} - \omega) \tag{4}$$

is the resonance detuning. A similar expression describes the inverse stimulated $2 \to 1$ transition. If the observation time (for which we also employ the term 'measurement time' in what follows) satisfies the condition $t \gg 1/\Delta$, the transition probability is proportional to the time [from here on, Δ is understood as the square root of the mean value $(\overline{\Delta^2})^{1/2}$]; when the observation time $t \approx \hbar/\Delta$, expression (3) implies that the probability of different values of Δ is distributed in accordance with the law

$$\frac{1}{\Delta^2}\sin^2\frac{t\Delta}{2} \tag{5}$$

about the most probable values

$$E_2 - E_1 - \hbar\omega = \hbar(\omega_{21} - \omega) \approx \frac{\hbar}{t}\,. \tag{6}$$

If the transition occurs in a constant field, i.e., $\omega = 0$ (then, $|E_2 - E_1| = \hbar\omega_{21}$), its probability is proportional to the interaction time t, provided that $\omega_{21}t \gg 1$. With the constraint $t\omega_{21} \approx 1$, this implies that the shorter the measurement time interval t, the greater the uncertainty in the measured energy difference, i.e.,

$$|E_2 - E_1| \sim \frac{\hbar}{t}\,. \tag{7}$$

Similar reasoning also leads to the uncertainty relation for the stimulated $2 \to 1$ transition.

Counting the time not from $t = 0$ but from $t = -\infty$ and introducing a multiplier $\exp(\lambda t)$, by way of similar calculations we arrive at the same results if we put $\lambda \to 0$ in the final expressions (adiabatic switching). In doing so, we must

replace t with δt in the above results. In this case, the energy–time uncertainty relation can be written as

$$|E_2 - E_1 - \hbar\omega| < \frac{\hbar}{\delta t} . \tag{7'}$$

Using this relation and the identity $\delta E = \mathbf{v}\,\delta\mathbf{p}$ and taking the momentum conservation law for the system $\delta\mathbf{p}_1 = \delta\mathbf{p}_2 = \delta\mathbf{p}$ into account, we obtain Bohr's expression, which establishes the relationship between the uncertainty of the measured momentum $\delta\mathbf{p}$ and the time interval during which the measurement is made [23],

$$(\mathbf{v}_2 - \mathbf{v}_1)\,\delta\mathbf{p} \approx \frac{\hbar}{\delta t} . \tag{8}$$

This relation is also valid for separate momentum components, i.e., for δp_x, δp_y, and δp_z. In nonrelativistic quantum mechanics, there is nothing to limit the velocity difference acquired in the act of measurement. That is why it is possible to determine the difference of particle momenta with any accuracy by letting the velocity difference tend to infinity.

But in relativistic quantum mechanics, the situation is radically different because there exists the limiting speed of interaction propagation — the speed of light. Proceeding from Bohr's relation [23], Landau and Peierls [24] hypothesized that the uncertainty relation of the form $\delta p\,\delta t \sim \hbar/c$ must be satisfied in the measurement (i.e., in the interaction of a particle with a measuring instrument) of a momentum $\mathbf{p}$ which lasts for a time interval δt. For relativistic particles, this relation can be rewritten as a relation between the uncertainty in the particle energy and the time of its measurement,

$$\delta E\,\delta t \approx \hbar . \tag{9}$$

Consequently, in some portion of the trajectory that the electron traverses in a time δt after the first scattering event, its energy is defined with the inaccuracy $\hbar/\delta t$. Such an electron, which is termed half-dressed [18], interacts with a substance differently than a dressed electron.

During its further motion, it is dressed, i.e., renormalized (see Refs [17, 18]), and the energy difference is emitted in the form of electromagnetic radiation into a light cone along the path of motion (see the figure in Ref. [18], which illustrates the aforesaid). The regeneration time or the electron dressing time is defined by the above uncertainty relation on assigning values to δE and $\hbar\omega$, the undressed-electron energy proving to be less than the dressed-electron energy.

As an illustration of the aforesaid, we can give an example from electrodynamics with the inclusion of a longitudinal density effect [7a]. Let an electron pass from one medium to another (for simplicity, transit to the medium from a vacuum). Clearly it then polarizes the substance of the medium and its mass changes. It is easy to perform the requisite calculations. When the particle velocity remains invariable in going from one medium to the other, we have

$$\Delta m_{\text{med}} - \Delta m_{\text{vac}} = -\left(\frac{mc^2}{E}\right)^2 \frac{e^2\omega_0}{c^3} , \tag{10}$$

where

$$\omega_0^2 = \frac{4\pi N Z e^2}{m} \tag{11}$$

is the plasma (Langmuir) frequency and Δm_{med} and Δm_{vac} are the corrections to the electron mass caused by the inclusion of radiative corrections in the medium and in the vacuum. If the electron momentum does not alter in the transit, the answer is somewhat different,

$$\Delta m_{\text{med}} - \Delta m_{\text{vac}} = -\frac{e^2\omega_0}{c^3} . \tag{12}$$

The adduced example of mass renormalization for a charged particle in the medium shows that the mass of a bare electron is smaller than the mass of a dressed one. To compensate for the mass loss in the medium, the electron should supposedly decelerate. Furthermore, it should also make up for the radiation energy loss, which also leads to deceleration.

It turns out [17–19] that it is experimentally possible to observe a half-dressed electron in a diversity of physical processes.

As an example, we consider the bremsstrahlung of a relativistic electron in a crystal [1, 2]. As noted above, it occurs throughout the coherence length, i.e., the radiating electron interacts simultaneously with all nuclei located throughout this length along its path, and the radiation intensity is proportional to the squared number of atoms in L_{coh}. We assume that at some point of the trajectory, the electron is scattered through an angle significantly greater than mc^2/E and escapes from the range of coherence length. In this case, the probability of radiation is no longer proportional to the squared number of atoms within the coherence length, with the consequent reduction of the probability of radiation. We can also state with assurance that repeated radiation, upon emission of the first photon (and transition of the electron to the bare state), is strongly suppressed: it takes some time (called the regeneration time) for the electron to recover its proper field. However, the moving electron can travel a large distance during the regeneration period and can even escape from the range of radiation formation (the higher its velocity, the sooner the escape). Hence, it follows that hard photons are emitted primarily in the initial portion of the trajectory, i.e., at the entry of the electron into the crystal. The higher the energy of the radiating electron, the stronger the manifestation of this effect. This effect was presumably discovered in experiments staged in CERN (see review [2], which discusses Uggerhøj's group's experiments in a crystal). We also note the theoretical work [19], which discusses the spatial–temporal evolution of a half-dressed particle in a plate with a thickness smaller than the coherence length. The authors point out a diversity of quantum-electrodynamic processes whereby electrons can be observed in a half-dressed state.

4. Modern investigations of radiative processes in an amorphous medium

4.1 Experiment

We have already mentioned in the Introduction that the experimental papers published in 1994–1996 [6, 8, 13, 14] aroused considerable excitement among experts in high-energy physics. The experimental research was conducted on two electron beams at the Stanford electron accelerator with the electron energies 8 and 25 GeV. A study was made of the suppression of the bremsstrahlung of photons with energies ranging from 0.2 to 500 MeV on carbon, aluminum, iron,

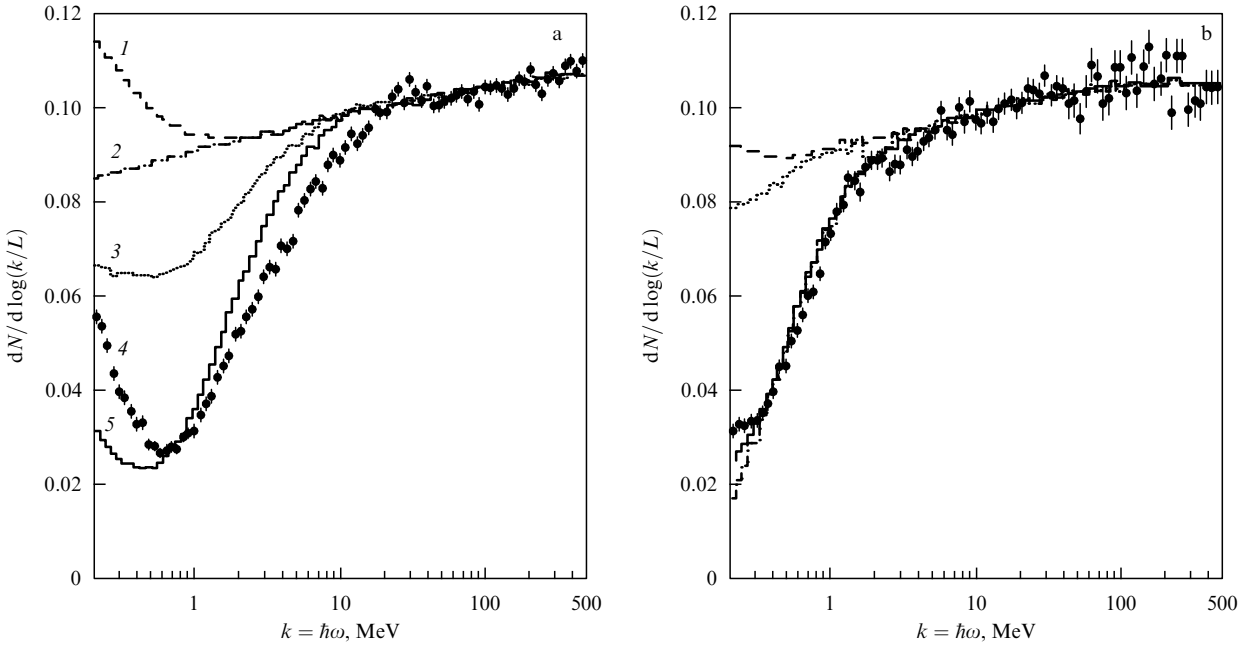

Figure 1. (a) 25-GeV electron emission spectrum multiplied by the photon energy $k = \hbar\omega$ in a carbon plate of thickness $2\%L$: *1* — BH + GF, *2* — BH, *3* — LP + GF, *4* (black points) — experiments with statistical errors, *5* — MC calculations with the inclusion of the suppression effects of LP, TM, and GF. (b) The same as in Fig. 1a for the electron energy 8 GeV. From top down, the curves correspond to the inclusion of the following processes: BH + GF, LP + GF. Plotted next are experimental points and the MC curve (the broken line), which includes only the BH + TM effects.

lead, tungsten, uranium, and gold targets of different thicknesses ranging from $0.1\%L$ to $7\%L$, where L is the radiation length. To avoid misunderstanding, we emphasize that the radiation length employed is a constant quantity that depends only on the medium characteristics (see Section 4.1).

The experiments were performed with high precision, which was far superior to the precision of all preceding experiments in this field. This enabled the authors to reconsider the results of previous investigations in this field, both theoretical and experimental.

The experimental data were compared with the curves (which modeled theoretical expressions) calculated by the Monte Carlo technique (hereinafter denoted by MC). The MC curves included the following effects: multiple scattering — the LP effect, dielectric suppression (i.e., the TM effect), the transition Ginzburg–Frank radiation (hereinafter GF) arising due to the existence of boundaries of the target samples, the photon absorption in the plate (the Galitskiĭ–Gurevich suppression effect), as well as the quality and internal structure of the target, multiple photon emission in the target, the experimental magneto-bremsstrahlung background arising in the deflecting magnets, etc.

The accuracy of experimental data processing was so high that they could be compared with various slightly different versions of the theory to within a few percent.

Beyond a doubt, the greatest difficulty consists of deciding between various versions of the bremsstrahlung theory for the MC curves because they are also only slightly different. Even if we consider formulas that have been used for a long time, like the Bethe–Heitler formula for the particle–atom bremsstrahlung, there is a need to improve the description of screening [25] and to include the contribution to the radiation made by atomic shell electrons for light atoms because the coefficient of the form $Z(Z+1)$ is now becoming unacceptable in view of the state-of-the-art accuracy and should be replaced with new expressions [6, 13].

The situation with other theoretical expressions employed in the SLAC E-146 Project is much more complicated. For instance, more than 50 years have passed since the publication of the well-known Ginzburg–Frank work [26] on transition radiation. In 1950–1970, the theory of this effect was substantially refined (account was taken of the effects of multiple scattering, plate thickness, oblique incidence, etc.). The works of that period were summarized in a monograph [1]. But some disagreement and unsolved problems still persist, influencing the comparison of theoretical results with experimental data (see below). Difficulties emerge in the selection of theoretical works on transition radiation in plates (with the inclusion of multiple scattering effects), because a wealth of papers whose data quite often contradict each other have come out. To construct the MC curves, the authors of Ref. [13] adopted the Pafomov version [27] for the portion where the transition radiation in the plate is significant.

As an illustration of the contribution of different suppression effects, in Figs 1a and 1b we compare the MC curves and the measured bremsstrahlung spectrum for electrons with the energies 8 and 25 GeV for a carbon target whose thickness is equal to 2% of the radiation length. We can see from Fig. 1a that the multiple scattering (LP) and longitudinal density (TM) effects make approximately the same contributions to the bremsstrahlung suppression; the growth in the left-hand side of the spectrum is due to the transition radiation (GF). For photons with energies far greater than 10 MeV, the experiment is described by the Bethe–Heitler expression. The discrepancy between the experimental data and the MC curve for photon energies below 1 MeV is attributed by the authors of Ref. [13] to the synchrotron radiation background. For an energy of the emitting electron of 8 GeV, the influence of the LP effect is weaker, because the ratio between the coherence lengths (for the same frequency of soft photon radiation) is proportional to the ratio between the squared

energies of the radiating particles, making the dielectric suppression (TM) the principal effect (Fig. 1b). Under these conditions, the growth of radiant energy at the left edge of the photon spectrum in Fig. 1a (which owes its origin to transition radiation) is hardly present in Fig. 1b. The suppression of transition radiation with lowering the incident particle energy (in the same frequency range) can supposedly be interpreted on the basis of a qualitative analysis. Indeed, we might assume that the effect of plate thickness on the total radiation is significant when this thickness is shorter than the coherence length. But our analysis shows (see below) that the stronger the inequality $l < L_{\rm coh}\omega/\gamma\omega_0$, the stronger the effect of thickness l. In this case, the total radiation and its frequency spectrum are significantly different. We consider this effect at the end of Section 4.4.

The authors of Ref. [13] note that the agreement between the experimental results and the theory is not as good as one might expect, although the experiments confirm the occurrence of suppression effects. In the above experiments with carbon, the authors point to material structural defects, whose inclusion is likely to improve the agreement with the theory. These issues are considered in Section 6.

The experiments performed on the SLAC are rich in data, and we restrict ourselves to the discussion of only some of them. The main results and their comparison with the theory are given in the figures in our review.

As noted above, the experiments performed in the framework of the SLAC E-146 Project enabled the authors of the experiment to discuss the theoretical research in detail. This was made possible by the high accuracy of the experimental works, which called for a more detailed consideration of the foundations of the theory.

4.2 Qualitative consideration

We now turn to the discussion of suppression processes in an amorphous medium. We discuss the suppression of bremsstrahlung in an amorphous medium caused by multiple electron scattering. As in the examples considered above, the bremsstrahlung is formed throughout the coherence length. But if multiple scattering deflects the radiating electron through an angle exceeding the characteristic angle of the bremsstrahlung, this results in a reduction of coherence length and hence in radiation suppression. A similar conclusion can also be reached by accounting for the longitudinal density effect (which amounts to the replacement of the speed of light in the vacuum with the speed of light in the substance), the photon absorption in the substance, and the effect of transition radiation. Evidently, a full account of theoretical works is not among the tasks of the author of this paper. However, gaining an understanding of the review by a wide circle of readers requires considering the theoretical foundations of all the indicated effects.

To estimate the bremsstrahlung cross section, we can use the Fermi – Weizsäcker – Williams method expounded in Section 6.1 as well as in Ref. [1, Sect. 2] for these purposes. It is well known that in the pseudo-photon method, the derivation of the bremsstrahlung formula amounts to the multiplication of the pseudo-photon flux corresponding to a single moving charged particle with the Klein – Nishina cross section and the subsequent integration of the resultant expression over the momentum transferred to the nucleus. The expression is of the form (see Ref. [1, formula (2.19)], in which we replaced $\delta = \delta_{\rm coh}$ with δ_2 to bring it into accord with expressions given below)

$$\mathrm{d}\sigma(\omega) = 2\bar{\sigma}\,\frac{\hbar\,\mathrm{d}\omega}{\pi\gamma}\int_0^{a/\hat{\lambda}}\mathrm{d}k_\perp\int_{\delta_2}^{k_1\,\max}\frac{k_\perp^2\,\mathrm{d}k_1}{k_1^2(k_1^2+k_\perp^2+R^{-2})^2}\times\left(1+\frac{\hbar^2\omega\delta_2}{m^2c^3}-\frac{2\delta_2}{k_1}+\frac{2\delta_2^2}{k_1^2}\right), \tag{13}$$

where

$$\bar{\sigma} = \frac{Z^2 r_0^2}{137} = Z^2\times 5.8\times 10^{-28}\ \mathrm{cm}^2\,,\qquad \hat{\lambda} = \frac{\hbar}{mc}\,,$$
$$a\approx 1\,,\qquad \gamma^{-2} = 1-\frac{v^2}{c^2}\,,\qquad r_0 = \frac{e^2}{mc^2}\,. \tag{14}$$

The integration of expression (13) with respect to $k_\perp^2 = k_2^2 + k_1^2$ should be extended only to values $a/\hat{\lambda}\approx mc/\hbar$, because the pseudo-photon method is inapplicable for distances shorter than the Compton wavelength of the electron. This is responsible for the logarithmic accuracy of the method. However, the simplicity of this method enables us to obtain estimates of many effects relatively easily, avoiding complicated mathematical calculations.

In expression (13), the main contribution to the integral over k_1 is made by the domain about the lower limit $k_1 \geqslant \delta_2$. If we integrate expression (13) with respect to the variable k_1 (taking into account that $\delta_2 = \delta_{\rm coh}$, with multiple scattering and the longitudinal density effect neglected) and then with respect to $k_\perp$, we obtain the Bethe – Heitler cross section with a logarithmic accuracy,

$$\mathrm{d}\sigma_{\rm BH} = 4\bar{\sigma}\left[\left(\frac{\hbar\omega}{E_1}\right)^2+\frac{4}{3}\left(1-\frac{\hbar\omega}{E_1}\right)\right]L_{\rm rad}\,. \tag{15}$$

In the case of total screening,

$$L_{\rm rad} = \ln\frac{aR}{\hat{\lambda}}-\frac{1}{2}$$

(see Ref. [1, Sect. 5]), where R is the atomic radius.

To include the LP and TM effects, we should proceed as follows: we use the expression for the minimal longitudinal momentum transferred to the atom, with multiple scattering and the longitudinal density effect taken into account,

$$\hbar\delta_2 = \hbar\delta_{\rm coh}-\frac{p_1\overline{\theta_1^2}}{2}-\frac{p_2\overline{\theta_2^2}}{2}+\frac{\omega(1-\sqrt{\varepsilon})}{c}\,, \tag{16}$$

where $\overline{\theta_{1,2}^2}$ are the mean squares of multiple scattering angles prior to and after the photon emission.

Approximately taking both effects into account leads to the following expression for the minimal momentum $\hbar\delta_2$ transferred to the medium, which determines the bremsstrahlung in an amorphous medium (for more details, see Ref. [1, Sect. 18]):

$$\delta_2\approx\delta_{\rm coh}+\frac{\delta_{\rm coh}}{m^2c^4}\frac{E_{\rm s}^2 l}{L}+\frac{\omega_0^2}{2\omega c}\,. \tag{17}$$

Here,

$$\delta_{\rm coh} = \frac{mc^2\hbar\omega}{2E_1E_2\hat{\lambda}} \tag{18}$$

is the minimal momentum (2), divided by $\hbar$, transferred to the medium in the bremsstrahlung, with the LP and TM effects ignored, which is inversely proportional to the coherence length (1), E_s is the multiple scattering constant equal to 21 MeV, L is the radiation length [see formula (23′) below], l is the length of particle trajectory through which coherent processes develop, $\hat{\lambda}$ is the Compton length of the electron divided by 2π, and ω_0 is the plasma frequency (11). Because l (as follows from Section 2) should be inversely proportional to δ_2, from expression (17) we obtain a quadratic equation whose roots define the effective value of δ_2 with the inclusion of both effects [11],

$$\delta_2 \approx \frac{1}{2}\left(\delta_{\text{coh}} + \frac{\omega_0^2}{2\omega c}\right) + \sqrt{\frac{1}{4}\left(\delta_{\text{coh}} + \frac{\omega_0^2}{2\omega c}\right)^2 + \frac{E_s^2 \delta_{\text{coh}}}{m^2 c^4 L}}\,. \quad (19)$$

In the absence of the LP effect, expression (19) gives the value of the minimal momentum transferred to the nucleus with the inclusion of only the TM effect,

$$\delta_2 = \delta_{\text{TM}} \approx \delta_{\text{coh}} + \frac{\omega_0^2}{2\omega c}\,. \quad (20)$$

When the longitudinal density effect can be neglected, from expression (19) we obtain a new value of the minimal transferred momentum associated only with multiple scattering:

$$\delta_2 = \delta_{\text{LP}} \approx \frac{\delta_{\text{coh}}}{2}\left[1 + \sqrt{1 + \frac{4E_s^2}{m^2 c^4 \delta_{\text{coh}} L}}\right]. \quad (21)$$

On substitution of (19) in (13), it is necessary to perform integration over the variables k_1 and $k_\perp$.

The expression for the bremsstrahlung cross section with the inclusion of only the density effect is rather easy to derive by replacing δ_2 with expression (20) and integrating similarly. The cross section for the emission of soft photons (i.e., $\hbar\omega \ll E_1$) then becomes [11]

$$\mathrm{d}\sigma_{\text{TM}} = \frac{16}{3}\,\overline{\sigma}\,\frac{\mathrm{d}\omega}{\omega}\,\frac{L_{\text{rad}}}{1 + (\omega_0^2/\omega^2)\,\gamma^2}\,. \quad (22)$$

The cross section in the limiting case with the inclusion of the LP effect is somewhat more difficult to obtain using the above expressions. For instance, we consider the emission of photons whose energies are far less than the initial energy of the radiating particle. In this case, $\delta_{\text{coh}} \approx m^2 c^3 \omega / 2E_1^2$, and it follows from (21) that δ_{LP} is given by the limiting expression

$$\delta_{\text{LP}} \approx \sqrt{\frac{\delta_{\text{coh}}}{L}}\,\frac{E_s}{mc^2} \approx \frac{E_s\sqrt{\omega}}{E_1\sqrt{2Lc}}\,. \quad (23)$$

In the cascade theory of showers, the path length z is commonly measured in t units,

$$t = \frac{z}{L}\,, \qquad \frac{1}{L} = \frac{4Z^2 r_0^2 N}{137}\ln\left(183 Z^{-1/3}\right). \quad (23')$$

The length L plays a significant part in the cascade theory of showers; prior to the discovery of suppression effects, it was believed to be a constant quantity. In reality, L is defined in terms of the Bethe–Heitler bremsstrahlung cross sections; because they vary if suppression effects are taken into account, L becomes dependent on the particle energy. That is why the cascade theory of showers should be formulated anew. However, in Refs [8, 9, 13, 14], which we here follow, the radiation length is considered to be the value of L with the suppression effects ignored. Another approach is used in Ref. [15], where an energy-dependent effective length is introduced.

The bremsstrahlung cross section takes the form [11]

$$\mathrm{d}\sigma_{\text{LP}} \approx \frac{4}{3}\,\frac{Zr_0}{137}\,\frac{mc^2}{E_1}\sqrt{\frac{L_{\text{rad}}}{2\pi c N}}\,\frac{\mathrm{d}\omega}{\sqrt{\omega}}\,, \quad (24)$$

where $L_{\text{rad}} \approx \ln\left(183 Z^{-1/3}\right)$ is the radiation logarithm.

Expression (24) differs from the exact Migdal formula [12] by the factor 1/3. We note that in three limiting cases, the above cross sections possess different emission photon spectra: those of Bethe–Heitler $\mathrm{d}\omega/\omega$, Landau–Pomeranchuk with the frequency dependence $\mathrm{d}\omega/\sqrt{\omega}$, and TM with the frequency dependence $\omega\,\mathrm{d}\omega$ for $\omega < \gamma\omega_0$. None of the formulas thus derived has the accuracy required for comparing the theoretical and experimental results [7–9, 13, 14]. But it is easy to see from these formulas that the multiple scattering and longitudinal density effects are responsible for a shortening of the coherence length, i.e., for the increase of the effective momenta transferred to the nucleus in the bremsstrahlung. This, in turn, leads to the suppression of bremsstrahlung, because the integral over the k_1 variable in expression (13) is determined by a domain about the lower limit. The last statement reflects the fact that high-energy processes possess a high directivity along the velocity of the process-initiating particle. That is why a simple introduction of the coherent length (1) on the basis of only the Heisenberg uncertainty relation $\Delta x \Delta p \approx \hbar$ (frequently used in the literature) would not suffice for the statement that high-energy processes are formed over long distances. For this statement to be legitimate, the main contribution to the cross section of the process should be made by reactions with small momenta k_1 imparted to the nucleus and aligned with the direction of radiating-particle motion. Expression (13) illustrates precisely this statement.

Obtaining more exact Migdal expressions [12] requires more tedious calculations. We do not reproduce these calculations here and refer to a monograph [1, Sects 18–21], in which the mathematical aspect of these investigations is expounded in sufficient detail.

We give the limits of the spectral ranges in which the limiting expressions for the bremsstrahlung cross section must be used. From expression (19), it follows that the limits of the Landau–Pomeranchuk range are determined by the inequality [11]

$$\frac{4E_s^2 \delta_{\text{coh}}}{m^2 c^4 L} \gg \left(\delta_{\text{coh}} + \frac{\omega_0^2}{2\omega c}\right)^2. \quad (25)$$

Inequality (25) implies the condition for the limits of the frequency range wherein the effect of multiple scattering is significant and the LP formula (24) is valid in the case where the energy of the emitted photon is far less than E_1,

$$\left[\frac{E_1^2}{E_s^2}\,\frac{L}{8\hbar c}\,(\hbar\omega_0)^4\right]^{1/3} \equiv \hbar\omega_1 \ll \hbar\omega \ll \hbar\omega_2 \equiv \left(\frac{E_s}{mc^2}\right)^2 \frac{8\hat{\lambda} E_1^2}{Lmc^2}\,. \quad (26)$$

Condition (26) determines the energy limit E_0 at which the LP effect occurs [11],

$$E_1 \geqslant E_0 = \frac{m^2c^4L\omega_0}{8cE_s}\,. \tag{27}$$

For dense media at the end of the periodic table of the elements, $E_0 \approx 1$ GeV.

The limits of the Bethe – Heitler range with the inclusion of the TM effect are defined simultaneously by two inequalities opposite to inequalities (26). One leads to the interval of emitted photon frequencies where the BH formula remains valid,

$$\frac{8c}{L}\,\frac{E_s^2E_1^2}{(mc^2)^4} \ll \omega \ll \frac{E_1}{\hbar} \tag{28}$$

and to the interval

$$\omega_{\rm at} \ll \omega \ll \left(\frac{L^{1/2}\omega_0^2}{2\sqrt{2c}}\,\frac{E_1}{E_s}\right)^{2/3}, \tag{29}$$

where formula (22) applies. The cross section is then defined by the BH formula if the condition

$$\omega > \gamma\omega_0 \tag{29$'$}$$

is satisfied, and by the TM formula otherwise.

In the derivation of conditions (28) and (29), it was assumed that the emitted photon energy is much lower than the energy of the radiating particle. For the emission of photons with an energy of the order of E_1, we should return to the investigation of expression (25) and write the condition ensuring that multiple scattering can be neglected as

$$4\left(\frac{E_s}{mc^2}\right)^2\frac{1}{L} \gg \delta\left(1+\frac{\omega_0^2E_1^2}{\omega^2m^2c^4}\right)^2. \tag{30}$$

(in the term related to the polarization of the medium, which is of significance only in the consideration of soft photons, E_2 can be replaced with E_1 [11]). The emission cross section throughout the emitted photon energy range (except for the LP range) is then defined by the expression

$$\mathrm{d}\sigma = 4\overline{\sigma}L_{\rm rad}\,\frac{\mathrm{d}\omega}{\omega}\left[\left(\frac{\hbar\omega}{E_1}\right)^2+\frac{4}{3}\left(1-\frac{\hbar\omega}{E_1}\right)\right] \times\left[1+\frac{\omega_0^2}{\omega^2}\left(\frac{E_1}{mc^2}\right)^2\right]^{-1}, \tag{31}$$

i.e., by the BH – TM formula [11]. For $E_1 < E_0$, only expression (31) holds true.

The spectral range wherein the LP formula is valid increases proportionally to the square of the initial energy of the radiating particle. However, it follows from condition (25) that the Bethe – Heitler expression remains valid for very hard photons in a very narrow photon energy range of the order of E_1. Formally, this amounts to replacing ω_2 with ω_2' in the right-hand side of (26),

$$\hbar\omega_2' \approx \frac{8c\hbar}{L}\left(\frac{E_s}{mc^2}\right)^2\frac{E_1E_2}{m^2c^4}\,. \tag{31$'$}$$

The monograph [1] gives the plot of the frequency dependence of the bremsstrahlung cross section under the condition

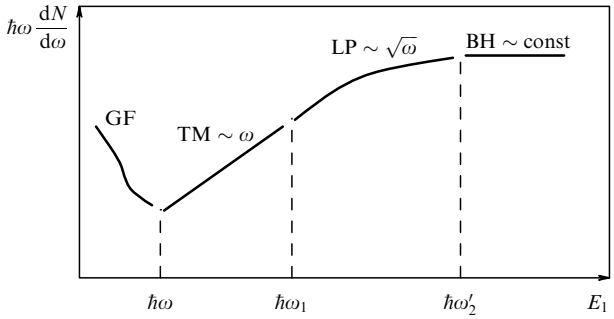

Figure 2. Bremsstrahlung spectrum, multiplied by the photon energy, as a function of the emitted photon energy. Indicated on the abscissa are the photon energy limits for different suppression ranges in arbitrary units. The plot is given for the energies

$$E_1 > E_0 = \frac{m^2c^3L\omega_0}{8E_s}\,,\quad \hbar\omega_1 \approx \left[\frac{(\hbar\omega_0)^4L}{8\hbar c}\,\frac{E_1^2}{E_s^2}\right]^{1/3},\quad \hbar\omega_2' \approx \frac{8c\hbar}{L}\,\frac{E_s^2E_1E_2}{(mc^2)^4}\,.$$

$E_1 < E_0$ and a plot borrowed from the reviews by E L Feĭnberg [12b] and by E L Feĭnberg and I Ya Pomeranchuk [12c], which shows the bremsstrahlung intensity (in terms of the BH units) as a function of the emitted photon energy (in terms of the E_1 units). Also given in Ref. [1] is the qualitative behavior of the differential energy loss by bremsstrahlung and pair production in relation to the parameter $\hbar\omega/E_1$, which was obtained in Ref. [28]. The aforesaid illustrates the simpler plot in Fig. 2, which is close to that given in Ref. [13].

To summarize the qualitative consideration of the effects of bremsstrahlung suppression in a homogeneous medium, we note that the characteristic parameter that determines the validity ranges for different bremsstrahlung formulas is the ratio between the right-hand side of inequality (26) and its left-hand side [11],

$$s' = \frac{mc^2}{E_s}\left[\frac{L\hbar\omega mc^2}{8E_1E_2\hat{\lambda}}\right]^{1/2}\left(1+\frac{\omega_0^2}{\omega^2}\right)\frac{E_1^2}{m^2c^4}\,. \tag{32}$$

In all subsequent versions of the theory, the quantity close to s' is conventionally denoted by s. The LP expression (24) is valid for $s \ll 1$, and the BH – TM expression (31) is valid for $s \gg 1$. This parameter (to a factor of the order of unity) also plays an important role in all subsequent theories.

4.3 Investigations of suppression processes in a semi-infinite medium

A B Migdal [12] considered the LP effect qualitatively by invoking his specially elaborated method for solving the kinetic equation, which he investigated in the Fokker – Planck approximation. He also included the longitudinal density effect and elaborated a quantum-electrodynamic theory. The Migdal bremsstrahlung cross section is defined by the expression

$$\mathrm{d}\sigma_{\rm br}^m = \frac{4}{3}\,\overline{\sigma}L_{\rm rad}\,\frac{\mathrm{d}y}{y}\left\{y^2G(s)+2\left[1+(1-y)^2\right]\Phi(s)\right\}, \tag{33}$$

where $y = \hbar\omega/E_1$, and the G and Φ Migdal functions are given in Migdal's work [12], as well as in Ref. [1]. For $s \gg 1$, the functions $G \to 1$, $\Phi \to 1$, and expression (33) becomes expression (31); for $s \ll 1$, it becomes expression (24) with a revised numerical coefficient. By replacing s with s' in (33), we

automatically take the longitudinal density effect in Migdal's theory into account.

Migdal's works performed for an infinite medium facilitated the rapid advancement of this direction and were expounded in Ref. [1, Sects 19, 20, supplements V–VIII]. Despite the long time that has elapsed after their publication, they underlie the processing of recent experimental data. The Migdal theory requires the introduction of an improved description of screening and the inclusion of radiation due to electrons following the prescriptions in Refs [6, 25], which was accomplished in Refs [8, 9, 13]. In this case, the Migdal expression assumes the form corresponding to that employed in Perl's works [6, 13],

$$\frac{\mathrm{d}\sigma_{\mathrm{MP}}}{\mathrm{d}k} = \frac{4\alpha r_{\mathrm{e}}^2}{3k}\left[\left\{y^2 + 2\left[1 + (1-y)^2\right]\right\}\left(Z^2 F_{\mathrm{el}} + Z F_{\mathrm{inel}}\right)\right], \quad (34)$$

where

$$F_{\mathrm{el}} \approx \ln\frac{184}{Z^{1/3}}, \quad F_{\mathrm{inel}} \approx \ln\frac{1194}{Z^{2/3}}, \quad \alpha = \frac{e^2}{\hbar c}, \quad r_{\mathrm{e}} \quad (35)$$

are the elastic and inelastic atomic form factors, the fine structure constant, and the electron radius, respectively.

Expression (34) was used in Refs [6, 8, 9, 13] in the processing of experimental data and is accurate to 2%, while Anthony et al. [13] believe that Migdal's formula (33) is accurate to 10%.

The qualitative analysis of the theory can be continued by extending it to a bounded medium, i.e., by including the GF transition radiation [26, 27] (see below). The photon absorption arising from pair production was taken into account in the Migdal theory by Galitskiĭ, Gurevich, and Yakimets [28, 29]. This proved to be significant at higher energies than in the experiments of Refs [8, 9, 13] (for instance, at energies of 10^{13} eV for lead). Ternovskiĭ [30] considered the pair production directly from electrons, although this process is still unlikely to make a tangible contribution to experimental results [6, 8, 9, 13]. Amatuni and Korkhmazyan [31] amplified the Migdal theory by accounting for the fuzziness of the boundary. They showed that the Migdal results remain in force when the thickness of the fuzzy boundary is less than the coherence length. The effects of target inhomogeneity, surface roughness, etc. are discussed in Section 6.

In the 1970s, a significant contribution to the LPM theory was made by Soviet theoretical scientists V Pafomov, I Toptygin, M Ryazanov, I Gol'dman, A Kalashnikov, F Ternovskiĭ, and others (see references in Ref. [1]). In connection with the publication of the experimental results of Refs [6, 8, 9, 13], new theoretical investigations have appeared, which we discuss briefly in Section 4.4.

The theory of transition radiation at the boundary between two media was first considered in the well-known paper by Ginzburg and Frank [26], to be further elaborated in a numerous publications. For the intersection of a vacuum–medium interface, the intensity of the GF transition radiation at normal incidence on the plate surface and for small radiation angles θ (counted from the direction of motion of the radiating particle) and high energies is given by the simple expression [1, formulas (26.17), (28.42), (28.42′)]

$$\frac{\mathrm{d}I_{\theta,\omega}}{\mathrm{d}\theta\,\mathrm{d}\omega} = \frac{2e^2}{\pi c}\,\theta^3\,\frac{\omega^2}{c^2}\left(l_{\mathrm{v}} - l_{\mathrm{m}}\right)^2. \quad (36)$$

Expression (36) involves the square of the difference of the coherence lengths in the vacuum l_{v} and in the medium l_{m} with the inclusion of medium polarization. Expression (36) is the relativistic limit of the GF formula [1, formula (24.22)]. The intensity of transition radiation is easy to estimate with the use of expressions for the coherence lengths in the first and second media. In the case of oblique radiation incidence on the surface, which has been considered by many authors, formulas (24.29)–(24.35) in Ref. [1] can be used. In this case, the transition radiation has two polarization components.

Integrating expression (36) over the angular variables, in the limit of frequencies exceeding the atomic frequencies, we obtain the expression for the intensity in the case of a single interface,

$$\mathrm{d}I_{\omega} = \frac{e^2}{\pi c}\left[\left(1 + 2\,\frac{\omega^2}{\omega_{\mathrm{cr}}^2}\right)\ln\left(1 + \frac{\omega_{\mathrm{cr}}^2}{\omega^2}\right) - 2\right]\mathrm{d}\omega, \quad (37)$$

in which we introduce, for simplicity, the notation

$$\omega_{\mathrm{cr}} = \gamma\omega_0, \quad (38)$$

where ω_0 is the plasma frequency in the plate, which has already been used in the discussion of the longitudinal density effect.

For $\omega \ll \omega_{\mathrm{cr}}$,

$$\mathrm{d}I_{\omega} = \frac{2\hbar}{137\pi}\,\mathrm{d}\omega\left(\ln\frac{\omega_{\mathrm{cr}}}{\omega} - 1\right). \quad (39)$$

For $\omega \gg \omega_{\mathrm{cr}}$,

$$\mathrm{d}I_{\omega} = \frac{\hbar\,\mathrm{d}\omega}{6\times 137\pi}\left(\frac{\omega_{\mathrm{cr}}}{\omega}\right)^4. \quad (40)$$

We integrate expression (37) over the frequency to obtain

$$I = \frac{e^2\omega_0}{3c}\,\frac{E}{mc^2}, \quad (41)$$

and therefore the energy of transition radiation at one interface is proportional to the particle energy [32a, b], which was borne out experimentally [33].

The situation radically changes when multiple scattering is taken into account in these expressions (see Refs [34–36] and also Ref. [1, Sects 26b, c, 28b, g]). This effect can be clearly understood from the following consideration. Formula (36) involves the squared difference of the coherence lengths in the vacuum and the substance. When suppression arising from multiple scattering is introduced into I_{c}, at frequencies exceeding the critical frequencies in the transition radiation, its intensity is nonzero. The spectrum of transition radiation then acquires new frequencies belonging to the range (26), and the radiated energy increases proportionally to E^2. This occurs when the radiating particle energy exceeds the energy E_0 introduced in the consideration of bremsstrahlung suppression. Formulas (37)–(41) change naturally in this case. The frequency and angular distributions of transition radiation then change accordingly (see Ref. [1, Sect. 26b and the example in Sect. 28]).

The effect of multiple scattering on the transition radiation has been studied since long ago. The first papers concerned with these subjects for a single interface were published in the 1960s and expounded in Ref. [1]. Garibyan and Pomeranchuk [34] were the first to point out this effect. Gol'dman [35a] later applied the Migdal theory in the

consideration of transition radiation at one interface between two media, and then Pafomov [35b] refined the results obtained.

I would like to emphasize that the formulas derived above for a semi-infinite medium cannot be applied to a plate with a finite thickness of the order of or smaller than $L_{\rm coh}$ by formally adding the transition radiation in the plate to the bremsstrahlung. Only the total radiation should be considered, including the bremsstrahlung and the transition radiation, as well as the interference term. In this case, the treatment is significantly complicated, while the radiation may be markedly different (see below). In the course of interaction with the radiating particle, the target plate of thickness l introduces a momentum uncertainty of the order of $\hbar/l$ along the direction of motion. When $l > L_{\rm coh}$, this uncertainty can be neglected in comparison with $\delta_{\rm coh}$. This implies that the plate sizes have no effect on the bremsstrahlung, i.e., the bremsstrahlung probability remains the same. Apart from the bremsstrahlung, the total radiation then also contains the transition radiation produced at the two plate boundaries (see below for the relative influence of multiple scattering). However, these questions have not been properly elucidated from the theoretical standpoint. The problem is that apart from transition radiation, the bremsstrahlung (with the inclusion of multiple scattering) is generated in the plate, which then interferes with the transition radiation. That is why there is no sense in separating the transition radiation from the total radiation (see the example at the end of the next section). Many experts took up this problem in the 1970s. To avoid misunderstanding, we emphasize that several papers resort to a coherence length definition more convenient for calculations, which is obtained by replacing $L_{\rm coh}$ with the coherence length and taking the dielectric suppression and the angle θ between the radiated photon and the electron into account,

$$L_{\rm f} = \frac{L_{\rm coh}}{1 + \gamma^2\theta^2 + (\gamma\omega_0/\omega)^2}\,. \tag{42}$$

Because there exist no generally accepted theoretical results on these subjects, the authors of Ref. [13] used the following procedure. To eliminate the effect of boundaries on the results of comparison with theoretical curves, a comparison was made of the difference of experimental data obtained with two plates of different thicknesses. With this procedure, the edge effects were suppressed and the agreement between experimental and theoretical data was substantially better.

4.4 Suppression of radiative processes in a plate

We now turn to the discussion of similar effects in a plate. The experiments at Stanford were performed on targets whose thicknesses ranged from 0.1 to 7% of the radiation length. The experimental data must therefore be compared with theoretical curves, with the transition radiation emerging in the plate (including multiple scattering) taken into account in addition to bremsstrahlung. The corresponding initial expressions for the probability of transition radiation at an incidence on a plate have been investigated by many scientists since the 1950s and are reviewed for normal incidence in Refs [36a – c]. The formulas required for the subsequent discussion are given in Ref. [1, Sect. 26]. For oblique incidence, the general solution was provided by Engibaryan and Khachatryan [37a], although this case has yet to be experimentally investigated in the transoptical spectral range and at ultrahigh energies (see Section 6.1). The corresponding results may be used in the investigation of nonuniform interfaces between two media (see Section 5.2).

In the limit of high energies and frequencies that exceed atomic frequencies, the spectral and angular intensity distribution in the case of normal incidence on a plate has the form (see Ref [2] or Ref. [1, formula (28.42)])

$$\mathrm{d}I^{(2)}_{\theta\omega} = \mathrm{d}I^{(1)}_{\theta\omega} \times 4\sin^2\left[\frac{\omega l_1}{2c}\left(1 - \frac{v}{c}\sqrt{\varepsilon_1}\cos\theta\right)\right]. \tag{43}$$

The second factor in formula (43) determines the interference between the radiation emerging at the two plate boundaries. It vanishes when the plate thickness l_1 is far less than the coherence length in the plate itself. But the contribution of transition radiation to the total radiation cannot be neglected for very thin plates because its intensity also vanishes when the plate thickness tends to zero. In the opposite case, this contribution is responsible for intensity oscillations. The position of maxima and minima is determined by the relation between the parameters appearing in the sine argument. The first factor in formula (43) describes the frequency – angular distribution of intensity at one interface between two media. The intensity of transition radiation at two interfaces is easy to estimate using the expressions for coherence lengths in the first and second media. The suppression of transition radiation in the plate differs from the above case of a semi-infinite medium with one boundary by the presence of the second factor in formula (43). It results in the additional suppression of transition radiation in comparison with the single-boundary case if the sine argument for high energies, small radiation angles, and high frequencies satisfies the condition

$$\left(1 - \frac{v}{c} + \theta^2 + \frac{\omega_0^2}{\omega^2}\right)\frac{\omega l_1}{c} \ll 1\,. \tag{44}$$

Ignoring the effect of multiple scattering, two main causes of suppression can be distinguished: the first is the finiteness of the trajectory in the target plate and the second is the longitudinal density effect. The transition radiation in the plate is suppressed by the one that leads to a stronger shortening of the coherence length.

Multiple scattering must be taken into account in the expression for the coherence length (see Ref. [1, Sect. 28b, g]). In this case, as for a single interface between two media, the spectrum of transition radiation, beginning with the energy E_0 introduced in Section 4.3, is enriched with photons lying in the energy range (26), their intensity in the bremsstrahlung radiation being determined by the cross section of the LPM effect. The situation is significantly complicated by the fact that the calculation of the radiation fields must include all processes that contribute to the radiation simultaneously. As a result, interference effects occur in the calculation of the total radiation intensity. In our case, these are given by the interference of the bremsstrahlung fields emerging in the plate itself (with suppression effects) and of the fields of transition radiation with the inclusion of multiple scattering. Pafomov [27] derived the formulas employed by the authors of Ref. [13] in the calculation of the MC curves for comparison with experiments on a plate. But this problem cannot be considered finally settled, although it has been the concern of numerous theoretical investigations performed, for instance, by Shul'ga and Fomin [38 – 43], Blankenbecler and Drell [44, 45], Zakharov [46, 47], and previously by Ternovskiĭ [30] and

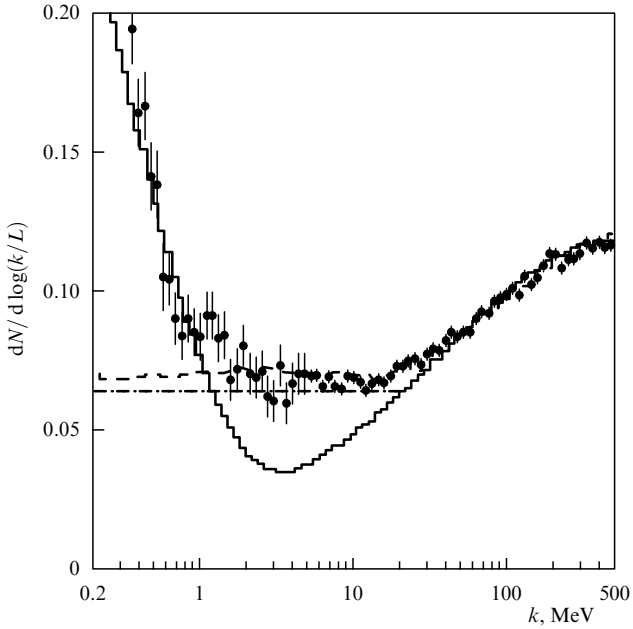

Figure 3. Emission spectrum of 25-GeV electrons in a gold plate of thickness 0.7%L. The zigzag solid line represents MC calculations [13] with the inclusion of the LP and TM suppression effects, as well as the transition radiation, following Pafomov. Experimental data (points) are given with statistical errors. The dashed and dash-dot lines were plotted using the calculated data from Refs [40] and [41], respectively (see text).

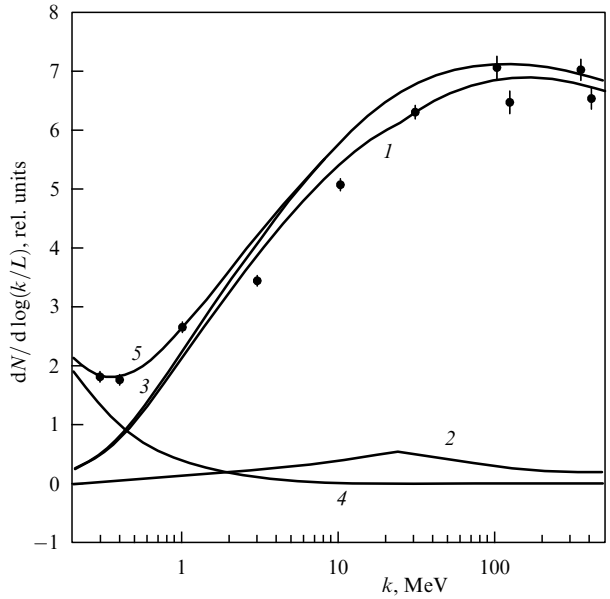

Figure 4. Curves calculated by Baĭer and Katkov [48] for a tungsten target with the thickness equal to 2%L and a radiating electron with the energy 2 GeV: curve *1* — the leading term comprising the LP + TM suppression; curve *2* — corrections related to the improved description of screening and a more rigorous calculation of the logarithmic term; curve *3* — the sum of the first two results; curve *4* — contribution of transition radiation; curve *5* — overall theoretical curve.

Pafomov [27, 36], and also the authors of works [1, Sect. 28b, g].

Shul'ga and co-authors [38] introduced the mathematical method of path integration into the bremsstrahlung theory, which made it possible to more correctly study the effect of multiple scattering on the radiative processes. Furthermore, they considered the effect of suppression [39–43] associated with the target thickness, which had been investigated by Ternovskiĭ [30] as early as 1960. Comparing the results of calculations and experiments [8, 9, 13] confirmed the conclusions reached in Refs [40, 44] and enabled reaching a theoretical explanation of the occurrence of the plateau discovered experimentally in the bremsstrahlung curve as a function of the emitted photon energy (Fig. 3).

Blankenbecler and Drell [44, 45] elaborated a quantum theory (a high-order eikonal approximation) for the investigation of bremsstrahlung suppression in an amorphous medium and for a plate. Their results for an infinite medium are similar to Migdal's results with an improved description of the screening. The results for a plate, which confirm the existence of a plateau, are shown in Fig. 3.

Using the path integration method, Zakharov investigated the LPM effect in the quantum electrodynamics approximation and obtained similar results [46]. Furthermore, in his next paper [47], he considered the radiation in a plate. Unfortunately, the authors failed to include the dielectric suppression in the three last-mentioned series of papers. That is why a comparison with the experiments of Refs [6, 8, 9, 13] was conducted only in that spectral range where the dielectric suppression is insignificant.

Baĭer and Katkov [48] solved the suppression problem of the ultrarelativistic particle bremsstrahlung in a plate with an accuracy exceeding the logarithmic Migdal accuracy by applying in quantum electrodynamics the quasi-classical operator technique developed by Novosibirsk theorists [49]. They investigated not only the effect of multiple scattering, but also the dielectric suppression. The effect of medium boundaries on the suppression processes, i.e., the transition radiation (see above), was considered and an improved screening was used in addition. Baĭer and Katkov [48] compared their results with the experimental data on tungsten (Fig. 4) and obtained good agreement throughout the emitted photon frequency range. Interestingly, the bremsstrahlung and the transition radiation produced at both target boundaries make equal contributions to the resultant radiation in the vicinity of the minimum. In addition to the overall theoretical curve, the partial curve corresponding to the contributions of different suppression effects is also plotted in Fig. 4.

Figure 5a, borrowed from Ref. [13], shows the results of experimental investigations and the theoretical MC curve for a very thin gold layer for the radiating particle energy 25 GeV. The transition radiation (in the range of experimentally measured frequencies) can be neglected. The LP effect can also be neglected, because the average multiple scattering angle is less than $1/\gamma$ and condition (27) should be fulfilled. Shown in Fig. 5b, borrowed from the same work, are similar data for the radiating particle energy 8 GeV. In this case, the LP range passing into the BH range should appear in accordance with inequality (26).

Baĭer and Katkov [50] considered the radiation in a gold plate with the aid of a specially elaborated method of calculation to obtain fairly good agreement with experiments. It must be noted that the authors of Refs [48–52] did not introduce special normalization factors in comparing their theoretical curves with the experimental ones from Refs [8, 9, 13], as was done in Ref. [13]. In my view, the theoretical Baĭer–Katkov investigation most thoroughly accounts for all suppression processes included in the total radiation amplitude. Consequently, accounting for the

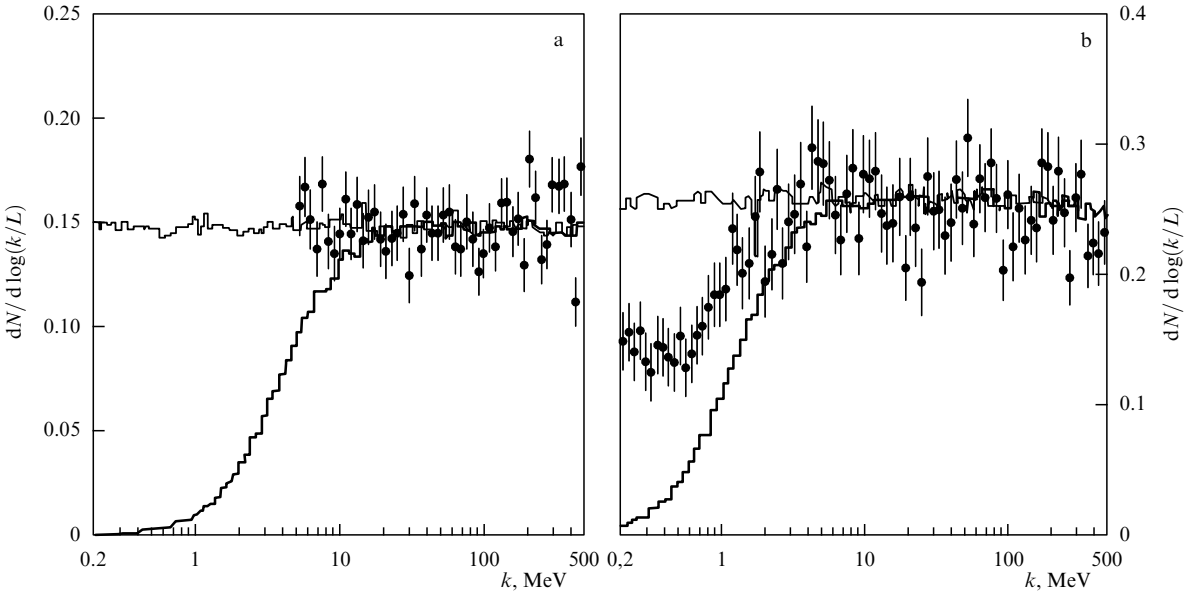

Figure 5. (a) Bremsstrahlung spectrum, multiplied by the emitted photon energy, for a gold plate. The plate thickness was only 0.1%L and the emitting electron energy was 25 GeV. The horizontal curve corresponds to the BH cross section and the solid zigzag curve corresponds to calculations including only the TM effect. (b) The same as in Figure a for an electron energy of 8 GeV.

interference of different channels that contribute to the overall emission plays a significant role in the calculation of the overall emission. This effect was predicted theoretically and observed experimentally in a different energy range. We turn to the discussion of this effect.

In a recent work [53] performed by Belgorod University physicists at the Kharkov electron accelerator, the bremsstrahlung of a collimated 150-MeV electron beam was investigated. The experiment was conducted with 50-μm thick aluminum plates. The results are shown in Fig. 6a. The transition radiation, the bremsstrahlung (with the nontrivial behavior of the TM density effect taken into account) and their interference are responsible for the oscillations of total radiation for photons with energies below 10 keV. This effect can be explained as follows [54]: the frequency – angular distributions of the transition radiation and the bremsstrahlung are different. An analysis shows [37b] that low scattering angles ($\theta \ll 1/\gamma$) make a small contribution to the transition radiation, which is mostly (over 90%) concentrated in the angular range

$$\frac{1}{4\gamma} \approx \theta \approx 4\left|\frac{1}{\gamma^2} + \frac{\omega_0^2}{\omega^2}\right|^{1/2} . \tag{45}$$

If the angular size of the collimated electron beam are bounded by a value $\theta_c \ll \gamma^{-1}$, the contribution of transition radiation becomes small and the influence of the LP effect is eliminated. The total radiation calculated in Ref. [54] is due to the contributions of the bremsstrahlung and the transition radiation, and their interference is responsible for the nontrivial behavior of the TM density effect and for the oscillations of the total radiation for photons with energies less than 10 keV. As a result, the authors derived the following expression for the radiation energy loss of the collimated electron beam in the frequency range dω [54]:

$$\omega \frac{\mathrm{d}N}{\mathrm{d}\omega} = \frac{e^2}{\pi}\, \gamma^2 \theta_c^2\, \frac{l}{l_0}\, \Phi(x, y) . \tag{46}$$

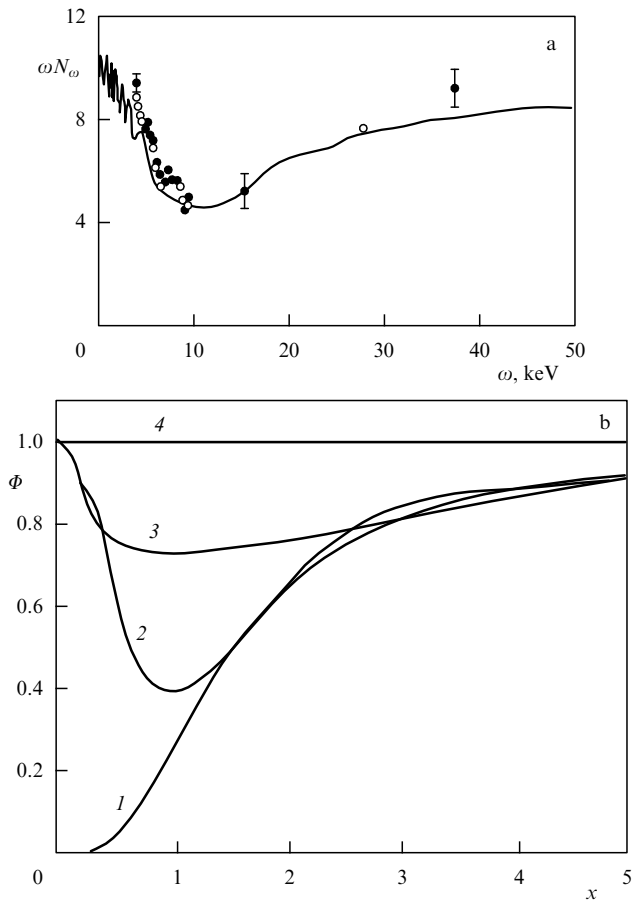

Figure 6. (a) Frequency dependence of the energy radiated by electrons in a thin (30 μm) aluminum plate. The electron energy was 150 MeV [53]. (b) Function Φ versus the $x = \omega/\gamma\omega_0$ variable for $y = \omega_0 l/2\gamma c = 1$ (curve *2*), $y = 5$ (curve *3*), and $y = 0$ (curve *4*). Curve *1* was plotted with the inclusion of the longitudinal density effect in a semi-infinite medium.

Here, $x = \omega/\gamma\omega_0$, $y = \omega_0 l/2\gamma c$, $l_0 = (mc^2/E_s)^2 l$, θ_c is the collimation angle, and the function $\Phi(x, y)$ (Fig. 6b) is defined by

$$\Phi(x, y) = 1 - \frac{2x^2}{(1+x^2)^2}\left(1 - \frac{\sin y(x+1/x)}{y(x+1/x)}\right). \tag{47}$$

The result in (46) is valid if two conditions are satisfied. The first follows from the requirement that the multiple scattering angles in the path length should be small in comparison with the characteristic radiation angles,

$$\overline{\theta^2} = \frac{E_s^2}{E^2}\frac{l}{L} < \gamma^{-2}. \tag{48}$$

It can be rewritten in a more convenient form as

$$l < \left(\frac{mc^2}{E_s}\right)^2 L = l_0. \tag{48$'$}$$

The second condition amounts to the requirement that the phase variation of the wave function of the radiating particle across its path length should be small. It leads to the constraint

$$l^2 \ll l_0 L_{\text{coh}} \tag{49}$$

on the path length. We note that in view of condition (48$'$), the target thickness can be greater or smaller than the coherence length.

The value of Φ as a function of x is plotted in Fig. 6b (curves *2* and *3*) for different values of y. Curve *1* corresponds to the longitudinal density effect for a semi-infinite medium and curve *4* to the case where the longitudinal density effect is absent. There is a certain analogy between the well-known Fermi density effect in the theory of ionization losses for a semi-infinite medium and its absence in a plate [55]. The difference is that the Fermi density effect operates perpendicular to the direction of particle motion, while the TM effect operates in the longitudinal direction. The results of the experiment and their comparison with the theoretical curve are given in Fig. 6a. It is significant that the soft photon emission intensity is nonzero, unlike the radiation in an infinite medium (i.e., with only one interface); in other words, the longitudinal density effect in a plate operates differently than in a semi-infinite medium.

5. Optical radiation of uniformly moving particles in inhomogeneous amorphous media

5.1 Optical radiation due to permittivity fluctuations

There is an intimate relationship between the in-medium light scattering and the corresponding charge particle radiation. By expanding the time-dependent electromagnetic field of a moving charge into a Fourier frequency integral and considering the interaction of individual frequency components (termed pseudophotons) with the substance, we actually reduce the problem of particle radiation to the problem of pseudophoton scattering. This method, proposed by Fermi–Weizsäcker–Williams, is used in what follows (for more details, see Section 6.1 or Ref. [1]).

The problems of light scattering in inhomogeneous media have been vigorously discussed in the literature, beginning with the first publications late in the 18th century and early in the 19th century and up to the present (see, for instance, Refs [56–58]). Any photon scattering process results in a similar pseudophoton scattering process, i.e., in charged particle radiation. It is beyond the scope of this paper to consider the problems of light scattering in any detail.

The radiation of relativistic particles in their passage through inhomogeneous amorphous media may be of immediate interest for the investigation of inhomogeneities themselves, even though their sizes may be far less than the sizes that are amenable to investigation in the scattering of photons of the optical range.

As shown below, the radiation of uniformly moving charged particles in the medium is expressed in terms of permittivity deviations from the average value. That is why all kinds of reasons or processes responsible for permittivity fluctuations (the fluctuations of thermodynamic parameters of the medium, medium inhomogeneities, surface roughness, etc.) result in radiation by the charges during their passage through the inhomogeneous substance.

The scattering properties of the medium are commonly characterized by the extinction coefficient $h(\omega)$, which is equal to the ratio of the number of scattered photons $\mathrm{d}m_{\mathbf{n}}$ (emitted by the moving charged particle) in the frequency interval $\mathrm{d}\omega$ over a unit path length in the direction of the vector $\mathbf{n}$ to the photon flux density $\mathrm{d}N(\omega)$ (pseudophoton flux density in the case of particles) in the frequency interval $\mathrm{d}\omega$ per 1 cm^2,

$$\mathrm{d}m_{\mathbf{n}} = h(\omega)\,\mathrm{d}N(\omega). \tag{50}$$

If the average value of the permittivity is denoted by ε_0 and its deviation (fluctuation) from the mean value by $\varepsilon'(\omega, \mathbf{r})$, the medium permittivity at each point is

$$\varepsilon(\omega, \mathbf{r}) = \varepsilon_0(\omega) + \varepsilon'(\omega, \mathbf{r}). \tag{51}$$

In what follows, the conditions

$$\varepsilon' \ll \varepsilon_0, \qquad \bar{\varepsilon}' = 0 \tag{52}$$

are assumed to be satisfied. We note that condition (52) is always satisfied for photons whose frequency is much higher than atomic frequencies.

The extinction coefficient is proportional to the mean value of the product of permittivity fluctuations at two different points integrated over the scattering volume and is usually written as

$$h(\omega) = \frac{\omega^4}{6\pi c^4}\overline{\int \varepsilon'(\mathbf{r}_1)\,\varepsilon'(\mathbf{r}_2)\,\mathrm{d}\mathbf{V}_{\mathbf{r}_1-\mathbf{r}_2}}. \tag{53}$$

For ideal gases, the permittivity fluctuation, which is determined by density fluctuations, is

$$\overline{\int \varepsilon'(\mathbf{r}_1)\,\varepsilon'(\mathbf{r}_2)\,\mathrm{d}\mathbf{V}_{\mathbf{r}_1-\mathbf{r}_2}} = \frac{4\left(\sqrt{\varepsilon_0}-1\right)^2}{N}, \tag{54}$$

where N is the number of atoms per 1 cm^3. In this case, upon multiplying $h(\omega)$ with the photon flux (the number of particles per square centimeter in a unit time), expression (53) describes the well-known Rayleigh law of light scattering in the atmosphere.

We multiply $h(\omega)$ with the total pseudophoton flux $\mathrm{d}N(\omega)$ in the frequency interval $\mathrm{d}\omega$ transferred by a uniformly moving particle across the plane perpendicular to the particle trajectory (for more details, see Section 6.1 and Refs [1, 61a]),

$$\mathrm{d}N(\omega) = \frac{1}{137\pi\beta^2\varepsilon_0^{3/2}}\,\frac{\mathrm{d}\omega}{\omega}\left[\ln\frac{q_{\max}^2 v^2}{\hbar^2|1-\varepsilon_0\beta^2|\omega^2} - \frac{v^2}{c^2}\,\varepsilon_0\right], \quad (55)$$

where $\beta = v/c$ is the particle speed expressed in terms of the speed of light and $h/q_{\max}$ is the minimal distance at which the macroscopic electrodynamics becomes applicable. We then obtain the number of photons radiated per unit particle path length [1, 59–61a] as

$$\mathrm{d}m = h(\omega)\,\mathrm{d}N(\omega)\,. \quad (56)$$

Expressions (55) and (56) determine the number of scattered photons for so-called distant encounters, for which the impact parameter is much greater than the interatomic distance. In this case, the angular distribution of the photons emitted per unit path length into a solid-angular interval $\mathrm{d}\Omega$ takes the form [59a, 61a] (see Section 6.1 as well as Ref. [1, formula (30.21)])

$$\mathrm{d}m_{\mathbf{n}} = \frac{3\,\mathrm{d}\Omega\,\mathrm{d}\omega}{16\times 137\times\beta^2\pi^2\varepsilon_0^{3/2}\omega}\left\{(1+\cos^2\theta)\right.$$
$$\left.\times\left[\ln\frac{q_{\max}^2 v^2}{\hbar^2\omega^2|1-\beta^2\varepsilon_0|} - 1\right] + 2(1-\beta^2\varepsilon_0)\sin^2\theta\right\}h(\omega)\,. \quad (57)$$

The problems of Rayleigh scattering polarization are discussed in Ref. [59a]. For short distances, the spatial dispersion of the permittivity must be taken into account, which automatically leads to cutting off the logarithm, for instance, at the Debye radius for a plasma [59b]. However, formulas (56) and (57) are somewhat modified in this case owing to the emergence of longitudinal waves in the plasma. The energy losses in statistically inhomogeneous media were considered in Ref. [59a].

I deliberately enlarged on the above example to emphasize the intimate relationship between charged particle radiation and the similar process of light scattering in inhomogeneous media.

5.2 Radiation at a rough interface

The problem that I attempt to discuss in greater detail here concerns the radiation of a charged particle in transit through the rough interface of two media. The statement of this problem is directly related to L I Mandel'shtam's work [58], who considered a similar problem of light scattering at a rough interface. We use the perturbation theory for simplicity [62]. Similar problems were considered more comprehensively in Ref. [63], including statistically rough interfaces. The corresponding experimental investigations performed by F Arutyunyan's group prior to 1969 were included in the monograph [1] (see also Ref. [64]).

We consider the radiation of a particle that crosses the interface of two media $z = f(x, y)$, where the function $f(x, y)$ defines the interface roughness (Fig. 7). In the first medium, $z < f$ and the permittivity is $\varepsilon_0(\omega)$; in the second medium, $z > f$ and the permittivity is $\varepsilon_0(\omega) + \varepsilon'(\omega)$.

The expression for the induction of the scattered field is of the form (see the derivation of expressions (58)–(61) in Section 6.1)

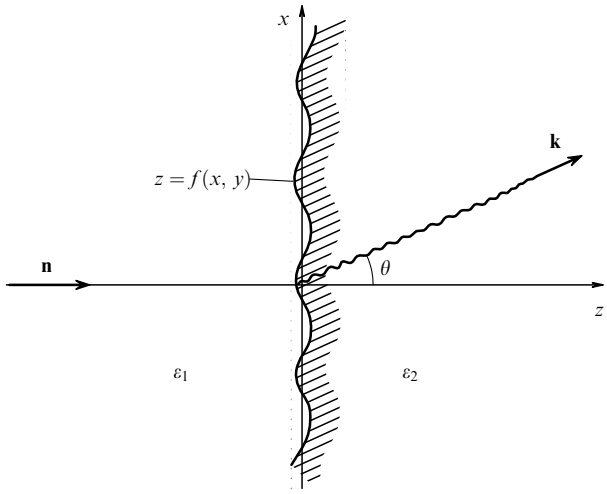

Figure 7. Photon emission at an angle θ to the z axis as a charged particle intersects the rough interface $f(x, y)$ of two media with permittivities ε_1 and ε_2.

$$\mathbf{D}'_\omega(\mathbf{r}) = -\frac{1}{4\pi}\left[\mathbf{k}'\left[\mathbf{k}', \int\frac{\mathbf{E}_{\omega 0}(\mathbf{r}_1)}{\mathbf{r}-\mathbf{r}_1}\,\varepsilon'(\mathbf{r}_1)\exp\left[\mathrm{i}\mathbf{k}'(\mathbf{r}-\mathbf{r}_1)\right]\mathrm{d}V_{\mathbf{r}_1}\right]\right], \quad (58)$$

where $\mathbf{k}' = (\omega/c)\sqrt{\varepsilon_0}\,\mathbf{n}$ is the wave vector of the emitted photon and $\mathbf{E}_{\omega 0}(\mathbf{r}_1)$ is defined by

$$\mathbf{E}_{\omega 0}(\mathbf{r}_1) = \frac{\mathrm{i}e}{2\pi^2}\int\int_{-\infty}^{+\infty}\int \mathrm{d}k_x\,\mathrm{d}k_y\,\mathrm{d}k_z\left(\frac{\omega\mathbf{v}}{c^2} - \frac{\mathbf{k}}{\varepsilon_0}\right)\exp(\mathrm{i}\mathbf{k}\mathbf{r}_1)$$
$$\times\left(k^2 - \frac{\omega^2}{c^2}\,\varepsilon_0\right)^{-1}, \quad (59)$$

with $\omega = \mathbf{k}\mathbf{v}$.

For convenience, we separate the factor depending on the variable z in expression (59) (the particle velocity $\mathbf{v}$ lies in the z axis):

$$\mathbf{E}_{\omega 0}(\mathbf{r}_1) = \exp\left(\mathrm{i}\,\frac{\omega}{v}\,z_1\right)\frac{\mathrm{i}e}{2\pi^2 v}\int \mathrm{d}k_x\,\mathrm{d}k_y\left(\frac{\omega\mathbf{v}}{c^2} - \frac{\mathbf{k}}{\varepsilon_0}\right)$$
$$\times\exp\left[\mathrm{i}(k_x x_1 + k_y y_1)\right]\left(k^2 - \frac{\omega^2}{c^2}\,\varepsilon_0\right)^{-1}$$
$$= \exp\left(\mathrm{i}\,\frac{\omega}{v}\,z_1\right)\mathbf{E}_\omega(x_1 y_1)\,. \quad (60)$$

For an arbitrary interface $z = f(x_1, y_1)$, the expression for the radiation field at a distance R_0 from the radiating object is of the form

$$\mathbf{D}'_\omega(R_0) = -\frac{\exp(\mathrm{i}k'R_0)}{4\pi R_0}$$
$$\times\left[\mathbf{k}'\left[\mathbf{k}', \int\mathbf{E}_\omega(x_1, y_1)\exp\left[\mathrm{i}\left(\frac{\omega}{v}\,k'_z\right)z_1\right]\right.\right.$$
$$\left.\left.\times\,\varepsilon'(\mathbf{r}_1)\exp\left[-\mathrm{i}(k'_x x_1 + k'_y y_1)\right]\mathrm{d}V_{\mathbf{r}_1}\right]\right]. \quad (61)$$

The formulas for transition radiation at one and two interfaces are the special cases of expression (61). For a single

boundary, we integrate over z_1 in expression (61) assuming that

$$\varepsilon'(\mathbf{r}_1,\omega)=\begin{cases}\varepsilon_1-\varepsilon_0\,, & -\infty<z_1<z=f(x_1,y_1)\,,\\ \varepsilon_2-\varepsilon_0\,, & z=f(x_1,y_1)<z_1<+\infty\,.\end{cases} \tag{62}$$

For normal incidence, when the particle velocity is perpendicular to the interface between two media [the plane $z=f(x_1,y_1)=0$], we obtain the following expression for the radiation intensity in the frequency interval $\mathrm{d}\omega$ and the solid angle $\mathrm{d}\Omega$:

$$\mathrm{d}I_{\omega,\mathbf{n}}=\frac{v^2e^2\sin^2\theta}{4\pi^2c^3\varepsilon_0^{3/2}}\,\mathrm{d}\Omega\,\mathrm{d}\omega \times\left|\frac{(\varepsilon_2-\varepsilon_1)(1-\beta^2\varepsilon_0-\beta\sqrt{\varepsilon_0}\cos\theta)}{(1-\beta^2\varepsilon_0\cos^2\theta)(1-\beta\sqrt{\varepsilon_0}\cos\theta)}\right|^2, \tag{63}$$

where $\beta=v/c$.

It turns out that in the perturbation-theory approximation, the sole formula (63) can be used to determine the emission into both the forward and the backward hemispheres, with the angle θ counted off from the plane $z=0$ and varied from 0 to π.

At normal incidence, when the interface is given as $z=x\tan\psi$ and the vector of particle velocity lies in the plane (x,y) at some angle ψ with the z axis, two polarizations are possible: the first with the electric vector lying in the emission plane (the plane containing the vector $\mathbf{k}'$ and the normal to the interface), and the second with the electric vector perpendicular to the emission plane. The polarization of the first type is termed parallel and is denoted by the superscript $\|$ and the polarization of the second type is termed perpendicular and is denoted by the superscript $\perp$. Therefore, the radiation intensity in the case of normal radiation incidence on the plane is

$$\mathrm{d}I^{\|}_{\omega,\mathbf{n}}=\frac{e^2\beta_z^2|\varepsilon_2-\varepsilon_1|^2\,\mathrm{d}\omega\,\mathrm{d}\Omega}{4\pi^2c\varepsilon_0^{3/2}\sin^2\theta_z\left|(1-\beta_x\sqrt{\varepsilon_0}\cos\theta_x)^2-\beta_z^2\varepsilon_0\cos^2\theta_z\right|^2} \times\left|\frac{(1-\beta_x\sqrt{\varepsilon_0}\cos\theta_x-\beta_z\sqrt{\varepsilon_0}\cos\theta_z-\beta_z^2\varepsilon_0)\sin^2\theta_z+\beta_x\beta_z\varepsilon_0\cos\theta_x\cos\theta_z}{1-\beta_x\sqrt{\varepsilon_0}\cos\theta_x-\beta_z\sqrt{\varepsilon_0}\cos\theta_z}\right|^2, \tag{64}$$

$$\mathrm{d}I^{\perp}_{\omega,\mathbf{n}}=\frac{e^2\beta_z^4\beta_x^2\cos^2\theta_y\varepsilon_0|\varepsilon_2-\varepsilon_1|^2\,\mathrm{d}\omega\,\mathrm{d}\Omega}{4\pi^2c\left|(1-\beta_x\sqrt{\varepsilon_0}\cos\theta_x)^2-\beta_z^2\varepsilon_0\cos^2\theta_z\right|^2\sin^2\theta_z} \times\left|1-\beta_x\sqrt{\varepsilon_0}\cos\theta_x-\beta_z\sqrt{\varepsilon_0}\cos\theta_z\right|^{-2}, \tag{65}$$

where

$$\beta_z=\beta\cos\psi\,,\qquad \beta_x=\beta\sin\psi\,,\qquad \cos\theta_x=\sin\theta\cos\varphi\,,$$
$$\cos\theta_y=\sin\theta\sin\varphi\,,\qquad \cos\theta_x=\cos\theta\,. \tag{66}$$

Here, φ is the angle between the x axis in the interface plane and the projection of the vector $\mathbf{k}'$ on this plane.

We finally give the formulas for the radiation intensity for a plate of thickness a. In lieu of the standard cumbersome expressions we have [compare with formula (43)]

$$\mathrm{d}I_{\omega,\mathbf{n}}=\mathrm{d}I_{\omega,\mathbf{n}}\left|1-\exp\left[\mathrm{i}\,\frac{\omega}{v}(1-\beta\sqrt{\varepsilon_0}\cos\theta)a\right]\right|^2 \tag{67}$$

for normal incidence and

$$\mathrm{d}I^{\|,\perp}_{\omega,\mathbf{n}}=\mathrm{d}I^{\|,\perp}_{\omega,\mathbf{n}}\left|1-\exp\left[\mathrm{i}\,\frac{\omega}{v_z}(1-\beta_x\sqrt{\varepsilon_0}\cos\theta_z-\beta_z\sqrt{\varepsilon_0}\cos\theta_z)a\right]\right|^2 \tag{68}$$

for oblique incidence.

The resultant formulas coincide with exact expressions (63) if the latter are expanded in terms of $\varepsilon_2-\varepsilon_1$ under the condition that

$$\cos^2\theta\gg\left|\frac{\varepsilon_2-\varepsilon_1}{\varepsilon_2+\varepsilon_1}\right|. \tag{69}$$

We note that the denominators of the above expressions may be equal to zero. This corresponds to the emergence of the Vavilov–Cherenkov radiation, whose intensity is proportional to the length of the particle path in the medium. The procedure of extracting the Vavilov–Cherenkov radiation from the above expressions was considered in Ref. [65].

We also note Ref. [66], where solutions were obtained for a large number of diverse interfaces between two media beyond the perturbation theory. Of special interest are statistically rough interfaces of two media [63], as well as interfaces of specially prescribed shapes, for which exact solutions have been found.

The above expressions can be extended to the range of hard photons, which allows investigating surface irregularities whose sizes are much shorter than the wavelengths of the optical range. No new experimental investigations have been carried out in this field. Staging experiments will undoubtedly result in advancement in this area. In my view, of special interest is the determination of the corresponding roughness in the nanostructural domain.

5.3 Using transition and diffraction radiation for diagnosing charged particle beams

In recent years, optical transition radiation (OTR) is surprisingly extensively used for the diagnostics of accelerated particle beams. The use of transition radiation for these purposes was first proposed by L Wartski rather long ago [67], but it has become an indispensable part of experiments only recently. This technique is employed to determine the geometrical (the profile, the divergence) and radiative parameters of charged particle beams in a wide energy range from 1 MeV to 30 GeV.

R Fiorito and W Rule [68] presented diverse theoretical calculations, which were experimentally confirmed, for the development of OTR detectors. The authors used them in the diagnostics of charged electron beams in the 17–110 MeV energy range. At present, OTR interferometers are used in wide ranges of radiating-particle energies and transition radiation wavelengths. They are the concern of numerous publications, which are referenced in Refs [69–73].

In his 2002 paper [74], R Fiorito summarized the long-standing OTR detector research. Everything actually reduces to the observation of the interference pattern of the two transition-radiation fields produced by bunch particles at two parallel metal foils separated by a distance l (compare with Fig. 8, in which the first perforated plate should be replaced with a continuous one). To calculate the optical transition radiation for relativistic energies and small scattering angles,

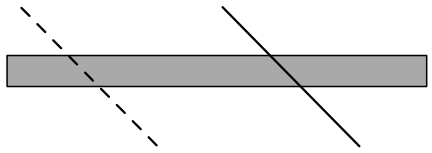

Figure 8. Schematic picture of the interferometer (Fiorito et al.) relying on the ODR – OTR interference. When the first plate is free from slots (is not perforated), we obtain the Wartski interferometer for measuring the angular divergence of a low-energy electron beam reliant on the interference of the OTR emerging at the two metal plates.

the formula similar to (43) can be used, with l_1 understood as the foil separation and $\mathrm{d}I^{(1)}_{\theta,\omega}$ as the intensity of transition radiation at a single interface. The beam characteristics can then be recovered by analyzing the interference pattern.

However, the situation in high-energy beam diagnostics has changed in the past few years. This is due to the following circumstances. Because the thin plates or foils, whose intersection by charged particle beams is accompanied by the generation of optical transition radiation, typically have edges, diffraction of pseudophotons of the particle electromagnetic field at the plate boundaries occurs in addition to the transition radiation (for more details, see below and the next section). This effect has been called the optical diffraction radiation (ODR) (see, for instance, Refs [1, Sect. 31; 75] and references therein), analogously to light diffraction. It is therefore no longer legitimate to determine the beam parameters at high particle energies using only the theory of transition radiation outlined in Section 5.1. This follows from the fact that the electromagnetic field of a moving relativistic particle decays over a distance ρ in the directions perpendicular to the particle velocity only when $\rho > \lambda\gamma$ (where λ is the wavelength of observed radiation and $\gamma^{-2} \approx 1 - \beta^2$ for $\beta = v/c \to 1$); at high energies, the particle field therefore elongates in the directions perpendicular to the direction of motion (see Section 6.1 and Fig. 8) to cross the plate edges. This gives rise to diffraction radiation.

Furthermore, in some cases, there is no way of using transition radiation at all, because the beam is subjected to deterioration as it passes through various obstacles. That is why a start has recently been made in applying nondestructive charged-beam diagnostic techniques involving the investigation of diffraction radiation. A comparative theoretical analysis of the characteristics of the diffraction and transition radiation was undertaken in Ref. [76]. The accomplishments in this area were summarized in Refs [77 – 82] and outlined in a recently published book [82], which includes references to the previous publications on these subjects.

The theory of diffraction radiation was developed by a number of well-known experts in 1950 – 1960. In several special cases, it has been possible to derive exact solutions. The results of that time were adequately covered in monograph [1]. In recent years, these problems have again come to the attention of physicists who study the properties of accelerated charged particle beams. A simple mathematical technique based on the Huygens method in electromagnetic wave diffraction theory, proposed in Refs [84, 85], is typically used in these investigations. We have already mentioned the analogy between the processes initiated by photons, on the one hand, and by charged particles on the other. The mathematical method based on this analogy is known as the pseudophoton method or the Fermi – Weizsäcker – Williams method [86 – 88]. The author has repeatedly used this method in the theories of bremsstrahlung, electron – positron pair production, diffraction radiation, etc. The pseudophoton method is considered in greater detail in Section 6.1.

Using the expressions given in Refs [84, 85, 1], Fiorito and his collaborators from Maryland University calculated and implemented a new OTR- and ODR-based type of interferometer, which is diagrammed in Fig. 8, borrowed from Ref. [77b]. If the first metal foil has openings, the diffraction radiation produced in it can interfere with the transition radiation produced by the beams in transit through the second metal plate. But if the electron undergoes scattering in its passage through the first plate, the interference effects vanish and the total radiation is given by the sum of OTR and ODR. In calculating the interferometer, Fiorito et al. used the approximate theory of diffraction radiation [84, 85] considered in Ref. [1] and based on the Huygens principle.

We briefly summarize the theoretical calculations. For the subsequent discussion, the expressions for the fields along ($E_\parallel$) and across ($E_\perp$) the direction of charge motion are required. We write the expression for the field of a fast charged particle Ze (Fig. 9) at a point $\mathbf{r}(vt, \boldsymbol{\rho})$ as

$$\mathbf{E}_\perp = \gamma \frac{Ze\boldsymbol{\rho}}{(\rho^2 + v^2t^2\gamma^2)^{3/2}}\,, \qquad E_\parallel = \gamma \frac{Zevt}{(\rho^2 + v^2t^2\gamma^2)^{3/2}}\,,$$
$$H \approx E\,, \qquad \beta = \frac{v}{c} \approx 1\,, \qquad E_\parallel \ll E_\perp \quad \text{for} \quad t_{\text{eff}} \approx \frac{\rho}{v\gamma}\,, \tag{70}$$

where

$$\gamma^2 = (1 - \beta^2)^{-1}\,. \tag{70$'$}$$

From expressions (70), it follows that the effective time of the interaction between the field of a particle Ze (for electrons, $Z = 1$ and $e = -|e|$) and an obstacle residing at a point $\mathbf{r}(vt, \boldsymbol{\rho})$ is $t_{\text{eff}} \approx \rho/v\gamma \approx (1 - \beta^2)^{1/2}\rho/v$. For $t < t_{\text{eff}}$, expressions (70) imply that $E_\perp \gg E_\parallel$, and the field of a fast moving particle acquires the properties of a plane electromagnetic wave

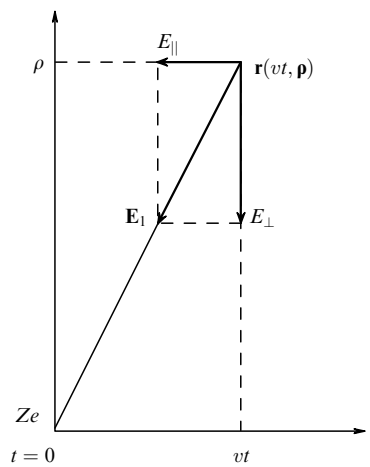

Figure 9. Electromagnetic field of a fast moving positive charge at a point $\mathbf{r}(vt, \boldsymbol{\rho})$, which is the location of an electron. The charge Ze is at the origin at a point in time $t = 0$ and travels along the vt-axis with a velocity $\mathbf{v}$ close to the velocity of light. The 'impact' time is $t_{\text{eff}} \sim \rho/v\gamma$. In this case, $E_\perp/E_\parallel \sim \gamma^2 \gg 1$ and the field of the fast moving charge acquires the properties of a plane electromagnetic wave compressed in the direction of motion of the particle Ze.

focused in the plane perpendicular to the direction of particle motion. It is easy to see that the temporal Fourier component $E_\perp(\omega)$ of the perpendicular component of the particle field $E_\perp$ is weak for $\rho > \hat{\lambda}\gamma$. This implies that the particle feels the obstacle (and accordingly experiences diffraction, i.e., emits pseudophotons) if the condition

$$\rho < \frac{\hat{\lambda}}{(1-\beta^2)^{1/2}} \tag{71}$$

is satisfied, where ρ is the distance between the particle trajectory and the obstacle at $t = 0$. The calculation of the diffraction radiation reduces to the calculation of the scattering of particle field pseudophotons from variously configured obstacles.

Simple expressions can be obtained with the use of the Huygens principle for the diffraction radiation intensity for a charged particle transiting through a round aperture or a slit in a screen. Naturally, the applicability conditions of geometric optics must be satisfied if the Huygens approximation is to be used,

$$\hat{\lambda} \ll a\,, \tag{72}$$

$$\theta \ll 1\,, \tag{73}$$

i.e., the emitted photon wavelength should be much shorter than the characteristic irregularity sizes and the photon scattering angles should be small.

We assume that the particle velocity is perpendicular to the screen plane. According to the Huygens principle, the total scattered field U (with U denoting the electric and magnetic components of the scattered field in what follows) is given by the integral taken over the area of a round aperture or slit,

$$U = \text{const} \int_{S_1} \frac{U^0(x,y)}{R} \exp\left(\mathrm{i}\,\frac{\omega}{c}\,R\right) \mathrm{d}S\,, \tag{74}$$

where R is the distance between the element of the aperture surface and the point of observation and U^0 is any of the monochromatic amplitudes of the particle field in free space without the time-dependent multiplier $\exp(\mathrm{i}\omega t)$.

An arbitrary point of the aperture is selected as the origin of the coordinates. Then,

$$R = |\mathbf{R}_0 - \boldsymbol{\rho}| \approx R_0 - \mathbf{n}\boldsymbol{\rho} + \frac{\rho^2}{2R_0}\,. \tag{75}$$

In the far-field (Fraunhofer) region, the second term in expression (75) can be neglected; in considering the near-field (Fresnel) region, it should be taken into account. From the total field, we subtract the field of a particle uniformly moving along the z axis

$$E^0_{x,y} = \frac{e\alpha}{\pi v} \exp\left(\mathrm{i}\,\frac{\omega}{v}\,x\right) \frac{(x,y)}{\sqrt{x^2+y^2}}\, K_1\left(\alpha\sqrt{x^2+y^2}\,\right), \quad \alpha > 0\,, \tag{76}$$

where K_1 is the Hankel function of the imaginary argument and $\alpha^2 = \omega^2/\gamma^2 v^2$, to obtain the resultant expression for the radiation fields for a round aperture

$$U(k_x, k_y) = -\frac{1}{(2\pi)^2} \int_{S_1} U^0(x,y) \exp(-\mathrm{i}\mathbf{k}\boldsymbol{\rho})\, \mathrm{d}S\,. \tag{77}$$

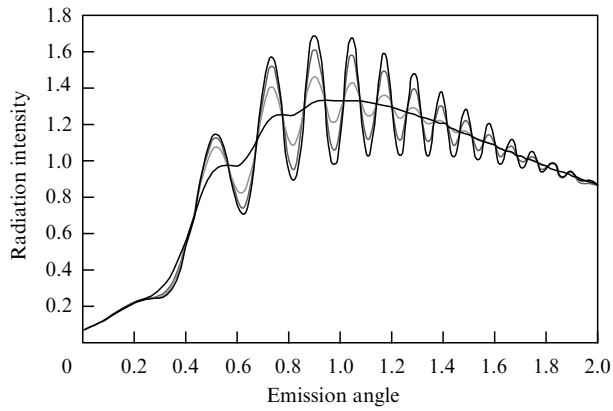

Figure 10. Radiation intensity (in terms of OTR) as a function of the emission angle (in units of γ^{-1}) for different angular divergences of the electron beam (from top down): 0.001 mrad, 1 mrad, 2 mrad, 4 mrad.

Here, the integral is taken over the entire z plane, except the round aperture area. In transit through a round aperture, the number of photons with a frequency ω emitted into an angular range $\theta\,\mathrm{d}\theta$ at a distance $\mathbf{r}_0$ from the aperture center is given by the formula

$$N_\omega\,\mathrm{d}\omega\,\mathrm{d}\theta = \frac{1}{137\pi}\,\frac{\theta^3\,\mathrm{d}\theta}{1-\beta^2+\theta^2}\left[J_0^2(qa) + \left(\frac{r_0}{a}\right)^2 J_1^2(qa)\right]\frac{\mathrm{d}\omega}{\omega}\,. \tag{78}$$

For $r_0 = 0$, the result coincides with exact calculations [90].

The corresponding formulas for the diffraction radiation in transit through a slit are given in Refs [84, 85; 1, Sect. 31]. The number of photons emitted into the frequency interval $\mathrm{d}\omega$ and the range of solid angles $\mathrm{d}\Omega$ is

$$\begin{aligned} N_\omega\,\mathrm{d}\omega\,\mathrm{d}\Omega = {} & \frac{e^2}{8\pi^2\hbar c}\,\frac{k^2}{f^2(f^2+k_y^2)} \\ & \times\Big\{(f^2+k_y^2)\left[\exp(-2fa_1) + \exp(-2fa_2)\right] \\ & - 2\,\frac{a^2\exp(-af)}{f^2+k_y^2}\left[(f^2-k_y^2)\cos ak_y - 2fk_y\sin ak_y\right]\Big\}\,\frac{\mathrm{d}\omega}{\omega}\,\mathrm{d}\Omega\,, \end{aligned} \tag{79}$$

where

$$\begin{aligned} & f = \sqrt{k_x^2 + a^2}\,, \\ & k_x = k\sin\theta\cos\varphi\,, \quad k_y = k\sin\theta\sin\varphi\,. \end{aligned} \tag{80}$$

Exact solutions were derived in Ref. [91].

The treatment of the problem of diffraction radiation in transit near a semi-infinite ideally conducting plane screen requires complex calculations with recourse to the Wiener–Hopf technique [92].

Using the above summary of theoretical results, R Fiorito and his collaborators from Maryland University calculated the radiation intensity in the ODR–OTR interferometer diagrammed in Fig. 8. Figure 10 illustrates the effect of charged-particle beam divergence on the interference pattern for the radiation emerging in the interferometer as a function of the observation angle. The electron energy was 8 MeV and the interferometer plate separation was 1.5 mm.

6. Radiation of hard photons in an inhomogeneous medium

6.1 Impact parameter technique

Of special interest is the possibility of producing hard photons as a charged particle uniformly moving along the z axis passes through inhomogeneous media [60, 61a]. We proceed from the macroscopic Maxwell equations for the potentials $\mathbf{A}$ and φ. For a more detailed consideration of the pseudophoton method, we give the corresponding equations that describe the fields $\mathbf{E}_\omega$ and $\mathbf{H}_\omega$ [61a], assuming that the particle travels along the z axis,

$$\begin{aligned}
&\operatorname{rot}\mathbf{E}_\omega = \frac{\mathrm{i}\omega}{c}\,\mathbf{H}_\omega\,,\\
&\operatorname{rot}\mathbf{H}_\omega = -\frac{\mathrm{i}\omega}{c}\,\varepsilon(\omega)\mathbf{E}_\omega\\
&\qquad\qquad + \frac{2e\mathbf{v}}{c}\int\delta(z-vt)\,\delta(x)\delta(y)\exp(\mathrm{i}\omega t)\,\mathrm{d}t\,,\\
&\operatorname{div}\varepsilon\mathbf{E}_\omega = \frac{2e}{v}\,\delta(x)\delta(y)\exp\frac{\mathrm{i}\omega z}{v}\,,\\
&\operatorname{div}\mathbf{H}_\omega = 0\,.
\end{aligned} \tag{81}$$

For $\varepsilon = \varepsilon_0 = \text{const}$, Eqns (81) constitute a well-known solution in the form of expression (59), where we should set $\omega = \mathbf{kv} = k_z v_z$. For convenience in the subsequent calculations, we separate the factor dependent on the variable z in expression (59). For the temporal Fourier component of the particle field, we then obtain expression (60) employed in Section 5.2. The density of the medium, along with the permittivity $\varepsilon(\omega, \mathbf{r})$, is assumed to vary only slightly in the direction of particle motion. This allows us to use the above expressions (51) and (52), which can always be fulfilled for the high frequencies under consideration, i.e., $\varepsilon' \ll \varepsilon_0, \bar{\varepsilon}' = 0$. In a similar way, it is also possible to introduce permeability for the description of inhomogeneous magnetic media and consider the radiation of transoptical frequencies at magnetic inhomogeneities. But to simplify the formulas, we restrict ourselves to the discussion of only electrical inhomogeneities, and do not touch upon the subject of scattered light polarization. We assign the zero subscript to all quantities in the zeroth approximation. The equations for the first-approximation fields, which are primed in what follows, can then be written as [61a]

$$\begin{aligned}
&\operatorname{rot}\mathbf{E}'_\omega = \frac{\mathrm{i}\omega}{c}\,\mathbf{H}'_\omega\,,\\
&\operatorname{rot}\mathbf{H}'_\omega = -\frac{\mathrm{i}\omega}{c}\,\mathbf{D}'_\omega\,,\\
&\operatorname{div}\mathbf{D}'_\omega = 0\,,\\
&\operatorname{div}\mathbf{H}'_\omega = 0\,.
\end{aligned} \tag{82}$$

The quantity $\mathbf{D}'_\omega$ involved in Eqns (82) is given by

$$\mathbf{D}'_\omega = \varepsilon_0\mathbf{E}'_\omega + \varepsilon'\mathbf{E}_{\omega 0} \tag{83}$$

and satisfies the equation

$$\Delta\mathbf{D}'_\omega + \frac{\omega^2}{c^2}\,\varepsilon\mathbf{D}'_\omega = -\operatorname{rot}\cdot\operatorname{rot}(\varepsilon'\mathbf{E}'_{\omega 0})\,. \tag{84}$$

The solution of Eqn (84) in the form of retarded potentials is given by formula (58). For convenience of calculations, we separate the factor dependent on the variable z in expression (59). We then arrive at expression (60). Because we have used macroscopic electrodynamics, Eqns (81) and (82) and expression (60) are valid at distances far exceeding the interatomic distance. To determine the radiated energy, $\mathbf{E}'^2_\omega$ should be averaged over the scattering volume.

We consider the fluctuations for which the correlation length (denoted by l_1) is of the order of the interatomic size. In this case, we have

$$\overline{\varepsilon'(\mathbf{r}_1)\varepsilon'(\mathbf{r}_2)} \neq 0 \tag{85}$$

for

$$|\mathbf{r}_1 - \mathbf{r}_2| \leqslant l_1\,. \tag{86}$$

Because expression (60) is valid for impact parameters that are significantly greater than the interatomic distance, in averaging $\mathbf{E}'^2_\omega$, we can take different $E_\omega(x_1, y_1)$ and $E_\omega(x_2, y_2)$ at the same point. For the radiated energy at distances R far exceeding l_1, the average value of the field $\mathbf{E}'^2_\omega$ scattered by the inhomogeneities of the medium is then given by

$$\begin{aligned}
\overline{\mathbf{E}'^2_\omega} = \frac{\overline{\mathbf{D}'^2_\omega}}{\varepsilon^2} = \frac{1}{16\pi^2R^2\varepsilon^2}\int\left|\left[\mathbf{k}'\left[\mathbf{k}'\cdot\mathbf{E}_\omega(x_1,y_1)\right]\right]\right|^2\mathrm{d}V_{\mathbf{r}_1}\\
\times\overline{\int\exp\left[\mathrm{i}\mathbf{k}'(\mathbf{r}_1-\mathbf{r}_2) - \mathrm{i}\,\frac{\omega}{v}(z_1-z_2)\right]\varepsilon'(\mathbf{r}_1)\varepsilon'(\mathbf{r}_2)\,\mathrm{d}V_{\mathbf{r}_1-\mathbf{r}_2}}\,.
\end{aligned} \tag{87}$$

We proceed from expression (87) to calculate the radiation intensity at large distances from the radiating object in the frequency interval $\mathrm{d}\omega$ and the range of solid angles $\mathrm{d}\Omega$. In this case, unlike analogous expressions considered in Section 5.1, expression (87) contains the additional factor

$$\exp\left[\mathrm{i}\mathbf{k}'(\mathbf{r}_1-\mathbf{r}_2) - \mathrm{i}\,\frac{\omega}{v}(z_1-z_2)\right]. \tag{88}$$

When the wavelength of the emitted photon is much longer than the characteristic inhomogeneity size and the particle velocity is close to the speed of light, the factor (88) is equal to unity. For the radiation of hard photons with the wavelength $\lambdabar$ much shorter than the characteristic inhomogeneity size l_1, the factor (88) can also be ignored provided the following two inequalities are satisfied:

$$\frac{\omega}{v}\left(1 - \frac{v}{c}\,\varepsilon_0^{1/2}\cos\theta\right)l_1 \ll 1\,, \tag{89}$$

$$l_1\,\frac{\omega}{c}\,\varepsilon_0^{1/2}\sin\theta \ll 1\,. \tag{90}$$

In this case, expression (55) for the pseudophoton flux transferred by a uniformly moving charged particle per unit path length, which is given in Section 5.1, and expression (57) for their angular distribution remain valid. Whenever any of inequalities (89), (90) is violated, the emission of hard photons is strongly suppressed.

Inequality (90) is fulfilled for hard photons emitted only at small angles θ relative to the direction of charged particle motion, because the emitted photon wavelength is significantly shorter than the characteristic inhomogeneity dimen-

sions of the medium,

$$\theta < \frac{\lambda}{l_1} \ll 1 . \tag{91}$$

With inequality (90) satisfied, inequality (89) leads to constraints for the interval of emitted frequencies,

$$\frac{2c}{l_1}\left(\frac{E}{mc^2}\right)^2 \gg \omega \gg \frac{l_1\omega_0^2}{2c} . \tag{92}$$

Condition (92) resembles a similar condition for the interval of emitted frequencies for small density variations in periodic media [60, 61a, b]. We substitute expression (60) in (87) and integrate the resultant expression with respect to k_x and k_y to obtain the angular distribution

$$I_{\omega\theta}\,\mathrm{d}\omega\,\mathrm{d}\Omega = \frac{l_1 e^2\omega^4}{32c^3\varepsilon^{3/2}\pi^3 v^2} \times \left\{(1+\cos^2\theta)\left[\ln\left(\frac{k_{\rho\,\max}^2 v^2}{\omega^2}\left(1-\frac{v^2}{c^2}\,\varepsilon\right)^{-1}\right)-1\right] + 2\sin^2\theta\left(1-\frac{v^2}{c^2}\,\varepsilon\right)\right\}\overline{\int \varepsilon'(\mathbf{r}_1)\varepsilon'(\mathbf{r}_2)\,\mathrm{d}V_{\mathbf{r}_1-\mathbf{r}_2}}\,\mathrm{d}\omega\,\mathrm{d}\Omega . \tag{93}$$

If inequality (90) is fulfilled, the integration should be extended to angles of the order of λ/l_1. We note that ideal gases obey formula (54). In this case, the number of emitted photons per unit path length in the frequency interval $\mathrm{d}\omega$ assumes the form [61a; 1, formula (30.24)]

$$I_\omega\,\mathrm{d}\omega \sim \frac{4r_0^2 Z^2 N}{137}\,\frac{\mathrm{d}\omega}{\omega^3}\,\frac{c^2}{l_1^2}\left\{\ln\frac{k_{\rho\,\max}^2 c^2}{\omega^2\left[1-v^2\varepsilon(\omega)\right]}-1\right\} . \tag{94}$$

Formula (94), as already noted in Ref. [61a], is little different from the corresponding formula for the number of emitted photons per 1 cm of path length in a stratified medium with a period l_1 and a small density variation if $N' \cong l_1^{-3}$,

$$\mathrm{d}m = \frac{16N'^2 Z'^2 r_0^2 c^2 l_1\,\mathrm{d}\omega}{137\pi\omega^3}\sum_{r=1}\frac{1}{r^3}\left[1-\frac{\omega l_1}{2\pi r v}\left(1-\frac{v}{c}\sqrt{\varepsilon_0}\right)\right] \tag{95}$$

[1, formula (28.77), in which the coefficient N' was missing] (see also Ref. [60, formula (19)]). The sum is practically determined by the term with $r = 1$. In actual practice, the Coulomb scattering of the radiating particle and strong density variations must be taken into account. This requires more complex estimates. Accelerator physicists have already encountered such problems. V A Verzilov, A P Potolitsyn et al. [93] recorded the radiation at macroscopic inhomogeneities in thin amorphous targets of aluminum and Mylar (see also Ref. [94]).

6.2 Comparison with resonance transition radiation

The previous review [2] was concerned with the Ginzburg–Frank transition radiation in periodic media (resonance transition radiation), which was intensively studied owing to its use in high-energy particle counters. In Refs [2; 1, Sect. 28f], an examination was made of the 'thermal background' in the resonance transition radiation emerging due to deviation of the medium structure from perfect periodicity. It is similar to the thermal background in coherent bremsstrahlung (ibid.).

For large deviations of the medium structure from periodicity, the bremsstrahlung cross section in a crystal is given by the standard Bethe–Heitler expressions summed over all atoms in the crystal. In the case of resonance transition radiation for large deviations from periodicity, we also obtain the sum of the transition radiation at individual plates [2].

The passage from the expressions for the radiation at periodic inhomogeneities to the expressions for the radiation at randomly located inhomogeneities in an amorphous medium is accomplished similarly. Using the expression for the number of emitted photons and the frequency intensity distribution of resonance transition radiation for a small density variation, Eqn (95), and comparing it with the corresponding expression (94) for an inhomogeneous amorphous medium, we can readily see the resemblance between them. This was already indicated when discussing formula (94). Therefore, we should probably not expect the total number of the emitted photons in a periodic medium to be significantly different from that in an amorphous medium with the same number of inhomogeneities per unit volume. Unfortunately, the theoretical treatment is extremely complicated when the density varies strongly from one random inhomogeneity to another.

In 1970–1975, the experimental investigation of radiation at high energies in inhomogeneous media was pursued by different scientific groups: F Arutyunyan of the Institute for Physical Research [95–98], M Lorikyan of the Yerevan Physics Institute [99, 100], L C L Yuan of the Brookhaven National Laboratory [101, 102], M Cherry of the E Fermi Institute, and others involved in cosmic ray research or working on large accelerators.

Figure 11a shows the results of measurements performed by F Arutyunyan's group [95, 96] to compare the intensities of 2.8-GeV electron radiation in a periodic medium and in an amorphous medium with numerically equivalent, randomly located inhomogeneities. Foam plastic was used as the inhomogeneous amorphous medium. The foam plastic density was equal to the 0.042 g cm^{-2} density of the periodic medium and its length was 1.74 times that of the periodic medium. The photon intensity radiated in the 15–240 keV energy range in the foam plastic proved to be 1.5 times lower than for the equivalent periodic medium. This work was performed in the Joint Institute for Nuclear Research (Dubna). M Lorikyan's group [99, 100] proposed a new type of a counter on the basis of their experiments. In the works of Yuan's group [101], measurements were made of 9.8-GeV electron radiation in a periodic stratified medium of aluminum plates situated in the air and in amorphous media with numerically equivalent inhomogeneities (Fig. 11b). In the works of M Cherry's group [103] performed at the Cornell synchrotron with 1–9 GeV electrons, investigations were made on various industrially produced foam plastics. Some of them proved to be suitable for use in transition radiation counters. The intensity of transition radiation in these foam plastics turned out to be similar to the resonance transition radiation in an equivalent stratified medium. The extensive experimental material of all investigations of that time was reviewed by F Arutyunyan and A Frangyan [104].

Unfortunately, there has been no major progress along this line of research during the last decades because of the difficulties encountered in staging experiments and the lack of new theoretical investigations in this field.

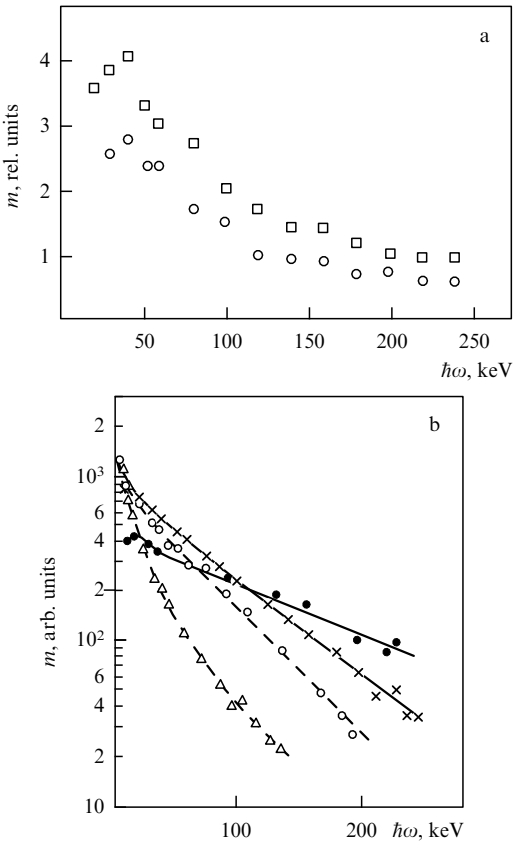

Figure 11. Comparison of the resonance transition radiation in a periodic medium and in a medium with numerically equivalent inhomogeneities (in this case, the boundaries between the inhomogeneities in the foam plastic). (a) 2.8-Gev electron emission spectra: □ — periodic paper – air stratified medium: the paper thickness $l_1 = 2.83 \times 10^{-3}$ cm, the number of layers $n = 2100$, the paper layer spacing $\alpha = 18.6 l_1$; ○ — inhomogeneous foam plastic medium: the density $\rho = 0.042$ g cm^{-2}, the foam plastic length $l = 202$ cm. (b) 9.8-GeV electron emission spectra: ● and × — aluminum – air ($l_1 = 2.54 \times 10^{-3}$ cm, $\alpha = 30 l_1$, $n = 231$) and Mylar – air ($l_1 = 2.54 \times 10^{-3}$ cm, $\alpha = 30 l_1$, $n = 231$) stratified media, respectively; ○ and △ — foam plastics with respective lengths $l = 12.7$ and 44.4 cm.

7. Conclusion

To conclude this review, we note that a number of issues in this area have not been covered. This applies primarily to nanostructure material research, which has attracted the attention of theorists and experimenters during the last decade, the theory of ionization losses in inhomogeneous media, and other related issues.

I would like to express my appreciation to numerous colleagues-physicists whose aid has been beneficial for the preparation of this review: M Perl and S Klein of Stanford University; V Baĭer and V Katkov of the Budker Institute of Nuclear Physics in Novosibirsk; R Fiorito of Catholic University of America in Washington, D.C.; N Shul'ga and S Fomin of the Institute of Physics and Technology in Kharkov; N Nasonov of Belgorod University; R Avakyan, S Darbinyan, and K Ispiryan of the Erevan Physics Institute; A Potolitsyn of the Institute of Nuclear Physics in Tomsk; I Dremin of the Physics Institute, Russian Academy of Sciences; A Frangyan of the Institute for Physical Research, National Academy of Sciences of Armenia; B Khachatryan of Erevan University, who familiarized me with some investigations in the area of radiative processes in inhomogeneous media. I would like to express my gratitude to the organizers of traditional conferences in Tomsk and Erevan, where some of the issues covered in this review were discussed at great length. Special thanks are due to E L Feĭnberg, from whom I derived major encouragement in the writing of the review. I am indebted to V Nikogasyan for his assistance in the preparation of the manuscript.

This work was supported by the INTAS-99-392 Program and the Ministry of Higher Education of Armenia (Grant No. 1350).

References

1. Ter-Mikhaelyan M L *Vliyanie Sredy na Elektromagnitnye Protsessy pri Vysokikh Energiyakh* (High-Energy Electromagnetic Processes in Condensed Media) (Erevan: Izd. AN Arm. SSR, 1969) [Translated into English (New York: Wiley-Interscience, 1972)]
2. Ter-Mikhaelyan M L *Usp. Fiz. Nauk* **171** 597 (2001) [*Phys. Usp.* **44** 571 (2001)]
3. Arutyunyan F R, Nazaryan A A, Frangyan A A *Zh. Eksp. Teor. Fiz.* **62** 2044 (1972) [*Sov. Phys. JETP* **35** 1067 (1972)]
4. Varfolomeev A et al. *Zh. Eksp. Teor. Fiz.* **69** 429 (1975) [*Sov. Phys. JETP* **42** 218 (1976)]
5. (a) Misaki A *Forschr. Phys.* **38** 413 (1990); (b) Polityko S et al., in *Proc. of the RIKEN Intern. Workshop on Electromagnetic and Nuclear Cascade Phenomena in High and Extremely High Energies, Tokyo, Japan, Dec. 22–24, 1993* (Eds M Ishihara, A Misaki) (Tokyo: RIKEN, 1994) p. 414
6. Perl M L, in *Les Rencontres de Physique de la Vallée d'Aoste: Results and Perspectives in Particle Physics, La Thuile, Aoste Valley, France, March 6–14, 1994* (Ed. M Greco) (Gif-sur-Yvette: Editions Frontieres, 1994) p. 567
7. (a) Ter-Mikhaelyan M L *Zh. Eksp. Teor. Fiz.* **38** 1167 (1960) [*Sov. Phys. JETP* **11** 845 (1961)]; Andreev I V *Zh. Eksp. Teor. Fiz.* **46** 1764 (1964) [*Sov. Phys. JETP* **19** 1188 (1964)]; (b) Baier V N, Katkov V M *Phys. Lett. A* **280** 275 (2001)
8. Anthony P L et al. *Phys. Rev. Lett.* **75** 1949 (1995)
9. Anthony P L et al. *Phys. Rev. Lett.* **76** 3550 (1996)
10. Landau L D, Pomeranchuk I Ya *Dokl. Akad. Nauk SSSR* **92** 535, 735 (1953)
11. Ter-Mikhaelyan M L *Dokl. Akad. Nauk SSSR* **94** 1033 (1954) [*Sov. Phys. Dokl.* **5** 527 (1954)]
12. (a) Migdal A B *Phys. Rev.* **103** 1811 (1956); Migdal A B *Zh. Eksp. Teor. Fiz.* **32** 633 (1957) [*Sov. Phys. JETP* **5** 527 (1957)]; (b) Feinberg E L *Usp. Fiz. Nauk* **58** 193 (1956); (c) Feinberg E L, Pomerančuk I J *Nuovo Cimento Suppl.* **3** 652 (1956)
13. Anthony P L et al. *Phys. Rev. D* **56** 1373 (1997)
14. Klein S "Suppression of bremsstrahlung and pair production due to environmental factors", Preprint No. 41350 (Berkeley, Calif.: Lawrence Berkeley National Laboratory, 1998)
15. Hansen H D et al. *Phys. Rev. Lett.* **91** 014801 (2003)
16. Feinberg E L, Preprint No. 166 (Moscow: Lebedev Physical Institute, 1972)
17. Feĭnberg E L, in *Problemy Teoreticheskoĭ Fiziki: Pamyati I E Tamma* (Problems in Theoretical Physics: In Commemoration of I E Tamm) (Ed. V I Ritus) (Moscow: Nauka, 1972) p. 110
18. Feĭnberg E L *Usp. Fiz. Nauk* **132** 255 (1980) [*Sov. Phys. Usp.* **23** 830 (1980)]
19. Fomin S P, Shul'ga N F *Phys. Lett. A* **114** 148 (1986)
20. Dremin I M, Lam C S *Mod. Phys. Lett. A* **13** 2789 (1998)
21. Kämpfer B, Pavlenko O P *Phys. Lett. B* **477** 171 (2000)
22. Ter-Mikaelyan M L *Usp. Fiz. Nauk* **167** 1249 (1997) [*Phys. Usp.* **40** 1195 (1997)]
23. Landau L D, Lifshitz E M *Kvantovaya Mekhanika: Nerelyativistskaya Teoriya* (Quantum Mechanics: Non-Relativistic Theory) (Moscow: Nauka, 1974) Sect. 44 [Translated into English (Oxford: Pergamon Press, 1977)]
24. Berestetskiĭ V B, Lifshitz E M, Pitaevskiĭ L P *Kvantovaya Elektrodinamika* (Quantum Electrodynamics) (Moscow: Nauka, 1989) [Translated into English (Oxford: Pergamon Press, 1982)]
25. Tsai Y-S *Rev. Mod. Phys.* **46** 815 (1974)
26. Ginzburg V L, Frank I M *Zh. Eksp. Teor. Fiz.* **16** 15 (1946)

27. Pafomov V E *Zh. Eksp. Teor. Fiz.* **47** 530 (1964) [*Sov. Phys. JETP* **20** 353 (1965)]
28. Galitsky V M, Gurevich I I *Nuovo Cimento* **32** 39 (1964)
29. Galitskiĭ V M, Yakimets V V *Zh. Eksp. Teor. Fiz.* **46** 1066 (1964) [*Sov. Phys. JETP* **19** 723 (1964)]
30. Ternovskiĭ F F *Zh. Eksp. Teor. Fiz.* **39** 171 (1960) [*Sov. Phys. JETP* **12** 123 (1961)]
31. Amatuni A Ts, Korkhmazyan N A *Zh. Eksp. Teor. Fiz.* **39** 1011 (1960) [*Sov. Phys. JETP* **12** 703 (1961)]
32. (a) Garibyan G M *Zh. Eksp. Teor. Fiz.* **37** 527 (1959) [*Sov. Phys. JETP* **10** 372 (1960)]; (b) Barsukov K A *Zh. Eksp. Teor. Fiz.* **37** 1106 (1959) [*Sov. Phys. JETP* **10** 787 (1960)]
33. Yuan L C L et al. *Phys. Lett. B* **31** 603 (1970)
34. Garibyan G M, Pomeranchuk I Ya *Zh. Eksp. Teor. Fiz.* **37** 1828 (1959) [*Sov. Phys. JETP* **10** 1290 (1960)]
35. (a) Gol'dman I I *Zh. Eksp. Teor. Fiz.* **38** 1866 (1960) [*Sov. Phys. JETP* **11** 1341 (1960)]; (b) Pafomov V E *Dokl. Akad. Nauk SSSR* **133** 1316 (1960)
36. Pafomov V E (a) *Zh. Eksp. Teor. Fiz.* **33** 1074 (1957) [*Sov. Phys. JETP* **6** 806 (1958)]; (b) *Izv. Vyssh. Uchebn. Zaved. Radiofiz.* **5** 1072 (1962); (c) Garibyan G M, Chalikyan G A *Zh. Eksp. Teor. Fiz.* **35** 1282 (1958) [*Sov. Phys. JETP* **8** 894 (1959)]
37. (a) Engibaryan V A, Khachatryan B V *Izv. Akad. Nauk Arm. SSR Fiz.* **1** 11 (1966); (b) Yan-Shi *Izv. Akad. Nauk Arm. SSR Fiz.* **9** 522 (1974)
38. Laskin N V, Mazmanishvili A S, Shul'ga N F *Dokl. Akad. Nauk SSSR* **277** 850 (1984) [*Sov. Phys. Dokl.* **29** 638 (1984)]
39. Shul'ga N F, Fomin S P *Pis'ma Zh. Eksp. Teor. Fiz.* **27** (2) 126 (1978) [*JETP Lett.* **27** 117 (1978)]
40. Shul'ga N F, Fomin S P *Pis'ma Zh. Eksp. Teor. Fiz.* **63** 837 (1996) [*JETP Lett.* **63** 873 (1978)]
41. Shul'ga N F, Fomin S P *Zh. Eksp. Teor. Fiz.* **113** 58 (1998) [*JETP* **86** 32 (1998)]
42. Shul'ga N F, Fomin S P *Nucl. Instrum. Meth. B* **145** 73 (1998)
43. Anthony P L et al. *Phys. Rev. Lett.* **75** 1949 (1995)
44. Blankenbecler R, Drell S D *Phys. Rev. D* **36** 277 (1987); **53** 6265 (1996)
45. Blankenbecler R *Phys. Rev. D* **55** 190, 2441 (1997)
46. Zakharov B G *Pis'ma Zh. Eksp. Teor. Fiz.* **63** 906 (1996) [*JETP Lett.* **63** 952 (1996)]
47. Zakharov B G *Pis'ma Zh. Eksp. Teor. Fiz.* **64** 737 (1996) [*JETP Lett.* **64** 781 (1996)]
48. Baier V N, Katkov V M *Phys. Rev. D* **57** 3146 (1998)
49. Baier V N, Katkov V M, Strakhovenko V M *Electromagnetic Processes at High Energies in Oriented Single Crystals* (Singapore: World Scientific, 1998)
50. Baier V N, Katkov V M, in *Quantum Aspects of Beam Physics: Advanced ICFA Beam Dynamics Workshop, Monterey, Calif., USA, 4–9 Jan. 1998* (Ed. P Chen) (Singapore: World Scientific, 1999) p. 525
51. Baier V N, Katkov V M, Strakhovenko V M *Nucl. Phys. B* **328** 387 (1989)
52. Baier V N, Katkov V M, Strakhovenko V M *Zh. Eksp. Teor. Fiz.* **94** 125 (1988); **36** 253 (1959) [*Sov. Phys. JETP* **94** 125 (1988); **9** 171 (1960)]
53. Arkatov U M et al. *Phys. Lett. A* **219** 355 (1996)
54. Nasonov N *Nucl. Instrum. Meth. B* **173** 203 (2001)
55. Ambartsumyan A S, Garibyan G M, Yan-Shi *Izv. Akad. Nauk Arm. SSR Fiz.* **16** (5) 343 (1981)
56. Cummins H Z, Levanyuk A P (Eds) *Rasseyanie Sveta Vblizi Tochek Fazovykh Perekhodov* (Light Scattering Near the Points of Phase Transitions) (Moscow: Nauka, 1990)
57. Fabelinskiĭ I L *Usp. Fiz. Nauk.* **164** 897 (1994) [*Phys. Usp.* **37** 821 (1994)]
58. Mandel'shtam L I *Polnoe Sobranie Trudov* (Complete Works) Vol. 1 (Ed. M A Leontovich) (Moscow: Izd. AN SSSR, 1948) p. 246; *Ann. Phys.* (Leipzig) **41** 609 (1913)
59. (a) Kapitsa S P *Zh. Eksp. Teor. Fiz.* **39** 1367 (1960) [*Sov. Phys. JETP* **12** 954 (1961)]; (b) Tamoĭkin V V *Izv. Vyssh. Uchebn. Zaved. Radiofiz.* **6** 257 (1963); (c) Tamoĭkin V V, Biragov S B *Zh. Eksp. Teor. Fiz.* **44** 1544 (1963) [*Sov. Phys. JETP* **17** 682 (1963)]; Kalashnikov N P, Ryazanov M I *Zh. Eksp. Teor. Fiz.* **45** 325 (1963) [*Sov. Phys. JETP* **18** 227 (1964)]
60. Ter-Mikhaelyan M L *Dokl. Akad. Nauk SSSR* **134** 318 (1960)
61. (a) Ter-Mikhaelyan M L *Izv. Akad. Nauk Arm. SSR* **14** 103 (1961); (b) Ter-Mikaelyan M L *Nucl. Phys.* **24** 43 (1961)
62. Ter-Mikhaelyan M L, Bagiyan R A *Dokl. Akad. Nauk Arm. SSR* **55** 32 (1979)
63. Bagiyan R A, Ter-Mikhaelyan M L *Zh. Eksp. Teor. Fiz.* **81** 1249 (1981) [*Sov. Phys. JETP* **54** 666 (1981)]
64. Arutyunyan F R et al. *Zh. Eksp. Teor. Fiz.* **77** 1788 (1979) [*Sov. Phys. JETP* **50** 897 (1979)]
65. Bagiyan R A *Izv. Vyssh. Uchebn. Zaved. Radiofiz.* **40** 1126 (1997)
66. Baghiyan R A *Phys. Rev. E* **64** 026610 (2001)
67. Wartski L et al. *Appl. Phys.* **46** 3644 (1975)
68. Fiorito R B, Rule D W, in *Beam Instrumentation Workshop* (AIP Conf. Proc., Vol. 319, Ed. R E Shafer) (Woodbury, NY: AIP, 1994) p. 21
69. Castellano M, Verzilov V A *Phys. Rev.: ST Accel. Beams* **1** 062801 (1998)
70. Catravas P et al., in *Proc. of the 1999 Particle Accelerator Conf., March 27–April 2, 1999, New York City, NY* (Piscataway, NJ: IEEE, 1999) p. 2111
71. Le Sage G P et al. *Phys. Rev.: ST Accel. Beams* **2** 122802 (1999)
72. Giove D et al., in *Proc. of the 3rd European Workshop on Beam Diagnostics and Instrumentation for Particle Accelerators: DIPAC97, Frascati, Italy, 12–14 Oct. 1997* (LNF-97/048(IR), Eds A Ghigo et al.) (Frascati: LNF, 1997) p. 251
73. (a) Artru X et al. *Nucl. Instrum. Meth. B* **145** 160 (1998); (b) Shul'ga N F, Dobrovol'skiĭ S N *Zh. Eksp. Teor. Fiz.* **117** 668 (2000) [*JETP* **90** 579 (2000)]
74. Fiorito R B, in *Electron-Photon Interaction in Dense Media* (NATO Science Series, Ser. II, Vol. 49, Ed. H Wiedemann) (Dordrecht: Kluwer Acad., 2002)
75. (a) Bolotovskiĭ B M, Galst'yan E A *Usp. Fiz. Nauk.* **170** 809 (2000) [*Phys. Usp.* **43** 755 (2000)]; (b) Bolotovskiĭ B M, Voskresenskiĭ G V *Usp. Fiz. Nauk* **88** 209 (1966) [*Sov. Phys. Usp.* **9** 73 (1966)]
76. Potylitsyn A P *Nucl. Instrum. Meth. B* **145** 169 (1998)
77. (a) Fiorito R B, Rule D W *Nucl. Instrum. Meth. B* **173** 67 (2001); (b) Shkvarunets A et al., in *2001 Particle Accelerator Conf.: PAC'2001, Chicago, IL, USA, June 18–22, 2001* (Piscataway, NJ: IEEE, 2001)
78. Shibata Y et al. *Phys. Rev. E* **49** 785 (1994); **50** 1479 (1994); **52** 6787 (1995)
79. Castellano M *Nucl. Instrum. Meth. A* **394** 275 (1997)
80. Artru X et al. *Nucl. Instrum. Meth. A* **410** 148 (1998)
81. Potylitsyn A P, Potylitsyna N A *Izv. Vyssh. Uchebn. Zaved. Fiz.* **43** (4) 56 (2000) [*Russ. Phys. J.* **43** 303 (2000)]
82. Vnukov I E et al. *Pis'ma Zh. Eksp. Teor. Fiz.* **67** 760 (1998) [*JETP Lett.* **67** 802 (1998)]
83. Wiedemann H (Ed.) *Electron-Photon Interaction in Dense Media* (NATO Science Series, Vol. 49) (Dordrecht: Kluwer Acad., 2002)
84. Ter-Mikhaelyan M L, Khachatryan B V *Dokl. Akad. Nauk Arm. SSR* **40** (1) 13 (1965)
85. Khachatryan B V *Izv. Akad. Nauk Arm. SSR Ser. Fiz.-Mat. Nauk* **18** (2) 133 (1965)
86. Fermi E *Z. Phys.* **29** 315 (1924)
87. Williams S *Kgl. Dan. Vidensk. Selsk. Mat.-Fys. Medd.* **13** 276 (1935)
88. von Weizsäcker C F *Z. Phys.* **88** 612 (1934)
89. Ter-Mikhaelyan M L *Izv. Akad. Nauk Arm. SSR* **9** (5) 77 (1956)
90. Dnestrovskiĭ Yu N, Kostomarov D P *Dokl. Akad. Nauk SSSR* **124** 1026 (1959)
91. Kazantsev A P, Surdutovich G I *Dokl. Akad. Nauk SSSR* **147** 74 (1962)
92. Sedrakyan D M *Izv. Akad. Nauk Arm. SSR Ser. Fiz.-Mat. Nauk* **17** (4) 103 (1964)
93. Verzilov V A et al. *Pis'ma Zh. Eksp. Teor. Fiz.* **65** 369 (1997) [*JETP Lett.* **65** 381 (1997)]
94. Platonov K Yu, Toptygin I N, Fleĭshman G D *Usp. Fiz. Nauk.* **160** (4) 59 (1990) [*Sov. Phys. Usp.* **33** 289 (1990)]
95. Arutyunyan F et al. *Dokl. Akad. Nauk Arm. SSR* **52** (4) 216 (1971)
96. Harutjunian F, Frangian A, Nazarian A, in *Cosmic Ray Conf. Papers: 12th Intern. Conf. on Cosmic Rays, Hobart, Tasmania, Australia, Aug. 16–25, 1971* Vol. 6 (Hobart: Univ. of Tasmania, 1971) p. 2469
97. Franghian A A et al. *Phys. Lett. B* **34** 227 (1971)

98. Arutyunyan F R, Ter-Mikhaelyan M L *Usp. Fiz. Nauk* **107** 332 (1972) [*Sov. Phys. Usp.* **15** 102 (1972)]
99. Lorikyan M P (a) *Prib. Tekh. Eksp.* **3** 73 (1971); (b) "Poteri energii v poristykh i sloistykh sredakh" ("Energy losses in porous and stratified media"), Abstract of Thesis for Doctorate of Physics-Mathematical Sciences (Dubna: Joint Institute for Nuclear Research, 1975)
100. Lorikyan M P, Shikhlyarov K K, Invention Certificate of the USSR, No. 304532; *Bull.* "*OIPOTE*" (17) 73 (1971)
101. Yuan L C L, in *Cosmic Ray Conf. Papers: 12th Intern. Conf. on Cosmic Rays, Hobart, Tasmania, Australia, Aug. 16 – 25, 1971* Vol. 4 (Hobart: Univ. of Tasmania, 1971) p. 1499
102. Yuan L C L et al. *Phys. Lett. B* **40** 689 (1972)
103. Prince T A et al. *Nucl. Instrum. Meth.* **123** 231 (1975)
104. Arutyunyan F, Frangyan A, Preprint No. 75-22 (Erevan: Institute for Physical Research, 1975)